

T-3679

**TITLE: FIELD EVIDENCE FOR THE ROLE
OF ORGANIC MATTER IN
DOLOMITIZATION**

by
Ronald J. Hill

ARTHUR LAKES LIBRARY
COLORADO SCHOOL of MINES
GOLDEN, COLORADO 80401

ProQuest Number: 10783433

All rights reserved

INFORMATION TO ALL USERS

The quality of this reproduction is dependent upon the quality of the copy submitted.

In the unlikely event that the author did not send a complete manuscript and there are missing pages, these will be noted. Also, if material had to be removed, a note will indicate the deletion.



ProQuest 10783433

Published by ProQuest LLC (2018). Copyright of the Dissertation is held by the Author.

All rights reserved.

This work is protected against unauthorized copying under Title 17, United States Code
Microform Edition © ProQuest LLC.

ProQuest LLC.
789 East Eisenhower Parkway
P.O. Box 1346
Ann Arbor, MI 48106 – 1346

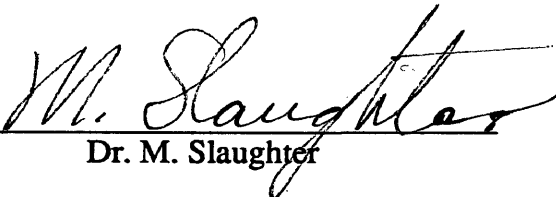
T-3679

A thesis submitted to the Faculty and Board of Trustees of the Colorado School of Mines in partial fulfillment of the requirements for the degree of Master of Science (Geochemistry).

Golden, Colorado

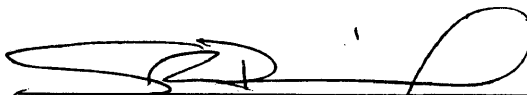
Date May 30, 1990

Signed: 
Ronald J. Hill

Approved: 
Dr. M. Slaughter

Golden, Colorado

Date May 30, 1990


Dr. S. R. Daniel
Professor and Head,
Department of Chemistry
and Geochemistry

ABSTRACT

Dolomite pods and thin laterally extensive, beds of dolomite in the Mississippian Madison Formation, a normal marine limestone, formed during early diagenesis in the zone of bacterial sulfate reduction or methanogenesis due to bacterial degradation of organic matter. The dolomite formed as a result of NH_3 produced by enzymatic protein hydrolysis and deamination during sulfate reduction or enzymatic protein hydrolysis and deamination coupled with CO_2 reduction during methanogenesis. The NH_3 acted to locally raise pH and thus, $\text{CO}_3^{2-}/\text{HCO}_3^-$ ratios in pore waters making dolomitization of the sediments favorable.

Physical evidence for the role of organic matter, and specifically, NH_3 in dolomitization is supported by the mineralogy and mineral composition of the Madison Formation. Authigenic NH_4^+ -illite and authigenic/detrital microcline, albite and quartz are present as accessory minerals. The illite contains NH_4^+ as interlayer cations and has an aluminum-rich, magnesium-poor octahedral layer indicating that the illite formed during sulfate reduction or methanogenesis, while NH_3 was produced from bacterial degradation of organic matter and magnesium was incorporated into dolomite. During intense sulfate reduction, most iron reduces and is incorporated into pyrite and carbonates, thus precluding the formation of illite and leaving microcline as the stable potassium/ammonium mineral. During less intense sulfate reduction, illite contemporaneous with dolomitization would retain Fe^{+3} but not magnesium. The Fe^{+3} content of Madison formation illites indicates reduction but not as intense as in the Green River Formation, where three layered clays reacted completely to form diagenetic sulfides and carbonates. Albite occurs

in all Madison samples to accommodate excess sodium and aluminum.

Carbon isotope values for limestones and dolomites are near the value estimated for Mississippian seawater, confirming that the dolomite of the Madison Formation formed by early diagenetic replacement. These values also indicate that carbon isotopes alone are not sufficient for determining the role of organic matter in dolomitization. Dolomites forming by direct precipitation from solution in the zone of bacterial sulfate reduction or methanogenesis in organic rich, detrital sediments show anomalously negative or positive carbon isotope values, respectively. The replacement dolomites of the Madison Formation show mineralogic evidence for formation in the zone of bacterial sulfate reduction or methanogenesis, but there is no carbon isotope evidence for direct precipitation. The carbon isotopes suggest dolomites precipitated directly from solution in organic rich, detrital sediments will have carbon isotope values reflecting the CO_3^{2-} carbon isotope value of the aqueous CO_3^{2-} whereas, dolomite formed by replacement in platform carbonates will have carbon isotope values reflecting the precursor carbonate mineral. Thus, consideration of sedimentary environment is important when interpreting carbon isotope values for dolomites. Mineral indicators may be more reliable than carbon isotopes for determining the role of organic matter in diagenesis and dolomitization.

The presence of organogenic dolomites in a normal marine environment suggests many platform and shelf dolomites could have an organogenic origin. The Madison Formation dolomites reflect zones where significant amounts of organic matter was initially preserved and suggests the laterally and vertically extensive dolomites that define the "dolomite problem" should be re-evaluated in light of these conclusions.

TABLE OF CONTENTS

	<u>Page</u>
✓ HYPOTHESIS: SULFATE-REDUCTION BY SULFATE-REDUCING BACTERIA IS THE CAUSE OF MUCH DOLOMITIZATION	2
DIAGENESIS OF CLAYS AND RELATED MATERIALS - THE EVIDENCE FOR ORGANICALLY INDUCED DOLOMITIZATION	5
PREVIOUS STUDIES	10
The Madison Formation	10
The Madison Formation near Lander, Wyoming	10
Dolomitization Models	11
Significance of Carbon Isotope Values for Dolomites	17
✓ Chemical Conditions needed for Dolomitization and the Significance of NH ₃	18
MADISON FORMATION CASE STUDY	20
Sampling	20
Sample Preparation	22
Quantitative Mineral Analysis	26
X-Ray Diffraction Analysis	26
Bulk Chemical Analysis	27
CO ₂ and H ₂ O Analysis	27
Chemical Analysis Problems Associated with QMAS	28
Mineral Nitrogen Analysis	29

Strontium Isotope Analysis	29
Carbon Isotope Analysis	30
Thin Section Analysis	30
Cathodoluminescence	30
RESULTS	32
✓ Bulk Mineralogy and Chemistry of Limestone and Dolomite Samples	32
Mineralogy and Chemistry of the less than one micron fraction for Limestones and Dolomites	37
Carbon Isotopes	37
Strontium Isotopes	43
Thin Section Analysis	43
Cathodoluminescence	44
INTERPRETATION	45
Chemistry and Mineralogy	45
✓ Dolomitization	48
Carbon Isotopes	50
Thin Section Analysis	52
Cathodoluminescence	52
Strontium Isotopes	53
✓ CONCLUSIONS	54
REFERENCES CITED	58
APPENDIXES	

A: Thin Section Descriptions	67
B: QMAS Theory	79
C: Mass Balance Calculations of Carbon Isotope Values in Organogenic Dolomites	87

LIST OF FIGURES

<u>Figure</u>		<u>Page</u>
1	Madison Formation Section near Lander Wyoming	22
1	Continued	23

LIST OF TABLES

<u>Table</u>	<u>Page</u>	
1	Sample location of limestone/dolomite pairs from Madison Formation, Wyoming	33
2	Bulk mineralogy of limestone samples (weight %)	34
3	Bulk mineralogy of dolomite samples (weight %)	35
4	Whole rock bulk chemistry of selected limestones and dolomites	36
5	Mineralogy of limestone less than one micron fraction from QMAS analysis	38
6	Mineralogy of dolomite less than one micron fraction from QMAS analysis	39
7	Bulk chemistry of the less than one micron fraction	40
8	Mineral nitrogen values and HN_4^+ to K^+ ratios for the less than one micron fraction	41
9	Carbon isotope values for some limestones and dolomites (Pee Dee Belemnite)	42
10	Calculated carbon isotope values in carbonate rocks for various amounts of organic matter and carbonate rock porosity for rock $\delta^{13}\text{C} = 1\text{‰}$	90
11	Calculated carbon isotope values in carbonate rocks for various amounts of organic matter and carbonate rock porosity for rock $\delta^{13}\text{C} = 3\text{‰}$	91

Acknowledgements

I am greatly indebted to Crystal Research Laboratories in Lander, Wyoming for doing bulk chemical analysis and CO₂/H₂O analysis which were used in QMAS to determine quantitative mineralogy of the limestone and dolomite samples. QMAS is available only at Crystal Research Laboratories. A special thanks to Ann Slaughter and Doug Wondrasek for carrying out these analyses and Ann O'Grady and Maynard Slaughter for assistance in QMAS determinations. I also, thank Crystal Research Laboratories for allowing me to use their x-ray diffraction unit to determine the mineralogy of my samples. Without the generous assistance of Crystal Research Laboratories and the people associated with this lab, the project would have been impossible to complete.

I am also, greatly indebted to Huffman Laboratories in Golden, Colorado for the generous discount given on mineral trace nitrogen analysis. Thanks to Ed Huffman and Dale Raines for the support. Without these analyses, the thesis would mean nothing.

Thanks to the Department of Chemistry and Geochemistry for financial support for two years and one field season while I was conducting this research. Thanks especially to Kata McCarville in the computing center for financial support my last semester. This support made life a lot easier.

Thanks to all my friends at the School of Mines for the fun and support - especially Don and Ed. Thanks to David Updegraf, Don Langmuir, Ron Klusman and David Budd (CU - Boulder) for their assistance and input in the project and to David Budd for obtaining the initial isotope data and cathodoluminescence. I am indebted to Dave Winter at UCLA for helping me with the rest of the isotope work. I am grateful to Maynard Slaughter, my

advisor on this project, for his assistance and guidance throughout and for the stimulating, thought provoking conversations while I was at the School of Mines. Without this, there would be no project and no degree.

Finally, thanks to my parents, Richard and Joan Williams and Jim Hill and the rest of my family for their continual support and love throughout my Master's program and my life. This could not have happened without all of you.

INTRODUCTION

Dolomite is a common mineral in the rock record, yet rare in recent sediments. Thermodynamically, dolomite is the stable carbonate in seawater, but calcite and aragonite preferentially precipitate. In an attempt to define the chemical parameters producing and inhibiting dolomitization, researchers have synthesized dolomite with varied results. Dolomite has been successfully precipitated in the laboratory at high temperatures ($> 150^{\circ}\text{C}$), but synthesis at lower temperatures ($< 100^{\circ}\text{C}$) has failed, preventing researchers from understanding the chemical and kinetic constraints controlling precipitation.

Numerous models for dolomitization have been proposed; however, no unifying theory exists to account for dolomite formation in contrasting environments. These models address mechanisms for supplying magnesium (Mg) to dolomitization sites, but do not consider detailed chemical aspects of dolomite formation. A unified theory should exist because dolomites are abundant and occur in varied environments. Almost all these environments have some common chemistry such as high pH and/or salinity and the presence of organic matter. These facts alone suggest a simple mechanism for most dolomitization.

Definition of a unified theory requires knowledge of the chemical parameters and processes favorable for dolomitization. Currently, no model attempts to qualify these constraints much beyond Ca/Mg ratios and Mg supply. If a unified theory is to be defined for dolomitization, the effects of CO_3^{2-} activity, pH, and salinity on carbonate precipitation must be considered and integrated.

The objective of this study is to obtain field data that will help researchers define the chemical parameters causing dolomitization and the role of organic matter in the dolomitization process. The hope is to correlate ammonia (NH_3) produced during enzymatic protein hydrolysis and deamination in a reducing environment with dolomitization. NH_3 will raise the pH and carbonate ion activity of a system, allowing dolomitization, provided an adequate magnesium source is present. A positive correlation between NH_3 production and dolomitization can be demonstrated by broadened kaolin x-ray peaks, high NH_4^+ content in diagenetic illites and/or illite-smectite mixed layer phases, ammonium-rich microcline or buddingtonite, and the association of minerals like pyrite, siderite, chlorite and organic matter within the dolomite. A positive correlation of NH_3 production and dolomitization would define chemical parameters favorable for dolomitization in natural systems beyond an adequate Mg supply or high salinity.

After presenting an hypothesis of dolomite formation and a summary of previous work done on dolomitization, an analysis of bulk mineralogy, less than one micron fraction chemistry and mineralogy, clay mineral compositions and carbon isotope data for samples collected for this study will be presented. From this data, interpretations and conclusions will be made in an effort to support or refute the hypothesis.

HYPOTHESIS: SULFATE REDUCTION BY SULFATE REDUCING BACTERIA IS THE CAUSE OF MUCH DOLOMITIZATION

The hypothesis of this study (Slaughter and Mathews, 1984) is that the decomposition of organic debris derived from plants, planktonic animals, and algae by bacteria in the zone of bacterial sulfate reduction, and specifically the enzymatic hydrolysis and deamination of

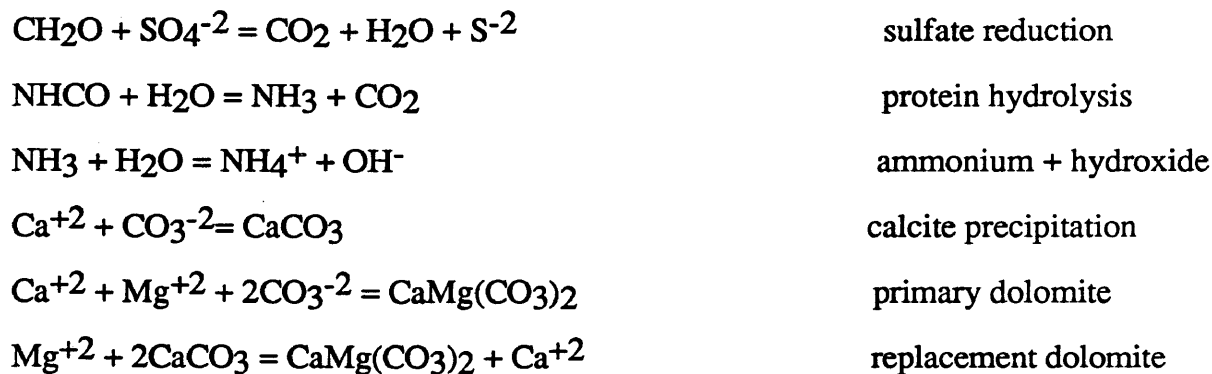
protein in this zone, is vital to much dolomitization. Several products of organic metabolism affect the solution chemistry to favor or inhibit dolomitization. The predominant products of organic metabolism in a reducing environment include CO_2 , H_2S , H_3PO_4 , NH_3 , humates and other weak organic acids and bases. Dolomitization is favored by high pH and/or salinity resulting in high carbonate ion (CO_3^{2-}) activity relative to bicarbonate (HCO_3^-) ion activity. Dolomitization is also favored by low sulfate (SO_4^{2-}) concentrations and the availability of Mg.

NH_3 produces high pH's. Decomposition of protein-rich organic matter in reducing environments produces relatively high concentrations of NH_3 and CO_2 along with H_2S . NH_3 is the only natural base strong enough and soluble enough to raise the pH in the presence of a variety of inorganic and organic acids in a closed system containing Types I and II kerogen or kerogen precursors. Increased pH from NH_3 release results in increased CO_3^{2-} activity. Extensive equilibrium calculations (Slaughter and Mathews, 1984) of simulated complex natural systems, using up to twenty acid-base and related reactions simultaneously, show the pH can rise to pH 11, when there is abundant protein in a reducing environment. Rosen, et al. (1988) reported measured pH's as high as 10 in a Coorong lake in South Australia, demonstrating that high pH's are attained in natural systems. NH_3 is not only a product of enzymatic protein hydrolysis and deamination during sulfate reduction, but is also a product of thermal organic decomposition at depth. NH_3 produced by pyrolysis will affect solution chemistry in a similar way to NH_3 produced by enzymatic hydrolysis and deamination during bacterial degradation of organic matter.

In the absence of high NH_3 in the sediment, salinity will control dolomitization or NH_3 and higher salinity will work together. High salinity produces increased carbonate ion

activities similarly to high pH. High salinity and high NH_3 production correlate, because the dominant organisms found in high salinity environments (algae and bacteria) are protein rich. There is also more sulfate (SO_4^{-2}) available for bacterial respiration.

Some important reactions, in very simple form, to consider are



Many dolomites formed in late diagenetic or epigenetic environments (Mattes and Mountjoy, 1980; Zenger, 1983; Gregg, 1985). According to the hypothesis given here, dolomitization can occur at any time organic nutrients and Mg are available. Thus, the hypothesis given here may be applicable to burial dolomites as well as early, near-surface dolomites. Ancient limestones could be dolomitized, particularly along fractures and other paths of higher permeability after burial, consolidation and uplift. In some cases burial dolomites may be more favorable for dolomitization than surface counterparts, as conditions necessary for dolomitization may not have existed during early diagenesis. Lastly, the hypothesis is consistent with the formation of such late dolomites as that associated with Missouri lead deposits formed in Ordovician beds during late Paleozoic times.

DIAGENESIS OF CLAYS AND RELATED MINERALS-THE EVIDENCE OF ORGANICALLY INDUCED DOLOMITIZATION

McHargue and Price (1982) and many earlier workers noted that dolomites are usually ferroan, argillaceous and appear to be diagenetic. Carbonate precipitation parallels the diagenesis of clays and other minerals. Clay mineral diagenesis begins soon after burial. Thus, clays coeval with dolomites should represent a record of the conditions present during diagenesis, and therefore, indicate conditions during dolomitization. Studies by Cooper and Evans (1983), Slaughter and Mathews (1984) and Cooper (1986) on the Green River Formation and studies by A.B. Carpenter (personal communication) on parts of the Miocene Monterey Formation of California, show that these two dolomite formations, originally protein rich, have abundant NH_3 and NH_4^+ in pore waters, organic matter and associated minerals.

If dolomites are diagenetic and a product of higher pH's, the composition of coeval clay minerals and related diagenetic minerals will reflect the pH's. During diagenesis, the formation of illite or the transformation of montmorillonite to illite or illite-smectite will be a significant process and reflect the NH_3 produced, and thus, high pH's by incorporating NH_4^+ into the illite interlayer cation sites substituting for K^+ . Clay formation or transformation is important as a diagenetic indicator, because the illitization process begins soon after burial, possibly within the first few meters of burial, as suggested by the work of Perry and Hower (1970) and Hower, et al. (1976). During the formation of illite from smectite, smectite layers collapse during diagenesis until approximately 50-60% illite is produced as a random mixed layer phase. At about 50-60% illite, recrystallization of the random mixed-layer phases to an ordered mixed layer phases begins and continues. The presence of random-mixed layer illite-smectite is not easily detected in x-ray diffraction

patterns until approximately 20% illite layers form. This may occur at shallow depths of burial. Because the transformation is a continuous process beginning very soon after burial, diagenetic conditions are continually recorded by the clays.

Since NH_4^+ follows K^+ geochemically, NH_4^+ is incorporated as an interlayer cation in diagenetic illites and illite-smectites during the transformation from montmorillonite layers (Stevenson and Dahriwal, 1959; Stevenson, 1962; Cooper and Evans, 1983; Slaughter and Mathews, 1984). NH_4^+ has also been reported in authigenic feldspars (Hallum and Eugster, 1976; Slaughter and Mathews, 1984). Ca^{+2} and NH_4^+ bind most strongly of the common exchange cations in zeolites and smectites. In a shallow, closed diagenetic, reducing system, NH_3 concentrations will be high in the sediment pore solution. Because of the strong binding of NH_4^+ in smectites, in a closed system NH_4^+ will remain in the diagenetic system. Thus, if NH_3 is produced, during protein metabolism and concurrently dolomitization, NH_4^+ should incorporate into diagenetic illite or illite-smectite. Similar results are expected at greater depths, where thermocatalytic NH_3 is produced.

In Paleozoic rocks, detrital sericitic illite derived from terrestrial mica sources is common. Diagenetic products of these illites must also be considered in the scope of this study. Sericitic illites are random mixed layer phases composed of 70-80% illite layers and 20-30% expandable smectite-like layers (Slaughter, personal communication, 1988). The expandable layers result from the substitution of Fe^{+3} and Mg^{+2} for Al^{+3} in the octahedral layer of the sericitic illite with substitution of Si for Al in the tetrahedral layer relative to smectite. These substitutions decrease layer charge, eventually producing expandable layers from originally nonexpanding layers. With diagenesis, the expanded layers associated with the sericitic illite will recollapse, with K^+ and NH_4^+ (if available) being incorporated as interlayer cations. The recollapsing of expandable layers will be a

continuous process beginning with early diagenesis, recording diagenetic conditions for dolomitization. The original sericite in this case will always have a high K^+ content and a relatively low NH_4^+ content.

Finally, a third type of diagenetic process may precipitate illite directly. The so called "ribbon illites" found in pore spaces of sandstones, specially treated to preserve the original texture, are of this type. These illites are diagenetically produced only and may contain mostly NH_4^+ as the charge balancing cation, if formed in the protein hydrolysis and deamination zone and less if NH_4^+ is formed during thermocatalytic organic degradation.

The diagenetic illites and mixed layer illite-smectites formed during dolomitization associated with sulfate reduction may show a lower iron and/or a lower magnesium content associated with reduction of iron by organic matter. Since bacterial protein degradation accompanied by sulfate reduction produces NH_3 instead of nitrate ions, Fe^{+3} will be reduced to Fe^{+2} (by H_2S), and enter sulfides, sedimentary chlorites and carbonates. Either low Fe^{+3} and more Fe^{+2} will occur in the octahedral layers of the three-layer clays or smectite-type clays, or there will be relatively large amounts of chlorite in contemporaneous carbonates.

Enzymatic protein hydrolysis and deamination and CO_2 reduction occurs during methanogenesis, which is the dominant bacterial process occurring in sediments after sulfate reduction ceases. NH_3 liberation and CO_2 reduction during methanogenesis will raise pH in this diagenetic environment, also, aiding dolomitization. Thus, NH_4^+ bearing diagenetic illites, illite-smectite would be expected in association with dolomite formed in either the sulfate reducing or the methanogenic zone.

Increases in pH due to NH_3 will significantly affect the crystallinity of clay minerals like those of the kaolin group. Kaolin allophane, an amorphous kaolin mineral with a

composition similar to kaolinite, becomes the stable phase at higher pH's (above about pH 8-9). At increased pH's, kaolin minerals act as weak Bronsted acids (due to the amphoteric nature of the kaolin minerals). The hydrogens that produce the well or poorly crystalline kaolin minerals through the regulation of the structure of the octahedral layer and hydrogen bonding between individual kaolin units at low pH's, are donated to the pore solution at higher pH's. This reduces hydrogen bonding between kaolin units and causes octahedral layer irregularities resulting in halloysite, the poorly crystalline kaolin mineral and eventually kaolin allophane with an amorphous structure. The presence of poorly crystalline kaolin minerals associated with the dolomites will be an indicator of pH conditions during dolomitization. An excellent example of kaolin allophane (amorphous kaolin) occurs as one of the abundant phases in the Green River Formation of the Piceance Creek Basin of Colorado (Slaughter and Mathews, 1984). Here mineral associations indicate pH's as high as 10-11.

There are problems with using kaolin minerals as pH indicators. Because the minerals are amphoteric, pH changes after dolomitization will change the kaolin crystallinity, possibly to better ordered forms if the pH decreases. This could occur if solutions move through the dolomite after dolomitization. Variations in pH conditions after dolomitization could make interpretation of pH conditions based on the crystallinity of kaolin minerals misleading. One should, when interpreting pH conditions using kaolin minerals, combine evidence from the kaolin mineral with other indicators such as NH_4^+ bound in other minerals to confirm the interpretation based on kaolin minerals.

There are economic implications for organically induced dolomitization. Kerogen, the insoluble precursor and product of oil and natural gas generation, is classified into three major types (Durand, 1980; Tissot and Welte, 1984). Type I kerogen comprises high

protein, paraffins (alkanes), carbohydrates, lipids, and aliphatic chains with few cyclic and aromatic compounds. Type I kerogen is derived mainly from protein-rich algal material. Type II kerogen comprises moderate amounts of lipids, proteins, aliphatic chains, naphthenic rings (saturated rings), some lignin, and carbohydrates. Type II kerogen derives mainly from mixtures of phytoplankton, zooplankton and microorganisms with some land plant material (lignin, etc.). Type III kerogen is composed of aromatic compounds, cellulose, phenols, and is low in aliphatic chains, protein and lipids. Type III kerogen derives primarily from terrestrial plants. Types I and II kerogen have high to moderate hydrocarbon generating capacities, respectively (Waples, 1985). The protein content of these types is high. Types I and II kerogen will, therefore, result in significant NH_3 production in a reducing environment, with Type I producing the largest concentrations.

If NH_3 is a vital component in dolomitization, the occurrence of dolomite will indicate not only diagenesis by sulfate reduction or methanogenesis, but also diagenesis by thermal decomposition when dolomite is a minor rock component. This implies that if appropriate burial depths have been reached, dolomitization coupled with clay diagenesis could be an indicator for oil generation and in the least, an indicator of kerogen-rich sediments, which upon thermal decomposition generate hydrocarbons.

There are other important implications: Mississippi Valley type mineral deposits such as the Missouri lead deposits may be formed by sulfate-reducing bacteria in a high protein, highly saline environment (Slaughter, personal communication, 1988).

PREVIOUS STUDIES

The Madison Formation

Mississippian strata in western Wyoming are dominantly carbonate deposits representing various depositional environments and have been defined as the Madison Group. Deposition of the Madison Group occurred from Kinderhookian to Meramecian time (Early to Late Mississippian). The Madison Group is divided into two formations, the Mission Canyon Limestone (upper Madison Group) and the Lodgepole Limestone (lower Madison Group). The Mission Canyon Limestone represents both open shelf and restricted shelf environments. Some gypsum and anhydrite rich intervals and solution collapse breccias are present along with some dolomite. The Lodgepole Limestone represents open shelf through shelf-margin environments. Thin to thick bedded limestones with variable amounts of dolomite comprise the Lodgepole Formation (Sando, 1976; Gutschick, et al., 1980; Budai, et al., 1987).

In the Wind River Basin, where samples for this study were collected, Mississippian sediments are defined as the Madison Formation. The Madison Formation is again divided into two units, the Upper Madison and the Lower Madison. The two units are separated by a disconformity marked by a limestone or dolomite breccia, cemented by a soft, argillaceous or silty dolomite. Normal marine microcrystalline limestones and bioclastic medium to coarse crystalline limestones with various amounts of dolomite dominate the limestones of the Madison Formation in the Wind River Basin (Strickland, 1957).

The Madison Formation near Lander, Wyoming

Paleogeographic reconstructions by Gutschick, et al. (1980) places the field area for this study (Sinks Canyon, near Lander, Wyoming and Limestone Mountain, at South Pass) in an open marine shelf to shelf margin environment. Field and thin section observations of

this study confirm these interpretations. In Sinks Canyon and at Limestone Mountain, Madison Formation sediments represent normal marine, near to outer shelf deposits, as is evident from the significant amounts of cross stratification and their shallowing-upward facies patterns (D. Budd, personal communication, 1988). Thin sections reveal a diverse fauna consisting of echinoderms, molluscs, brachiopods, arthropods, corals, foraminifera and algae consistent with a normal marine environment. There is no evidence of evaporites, further supporting a normal marine depositional environment in the study area around Lander, Wyoming. The normal marine interpretation for the Madison Formation in the study area rules out dolomitization in a high salinity, sabkha type environment and thus, makes the Madison Formation an excellent unit to test the ammonia hypothesis.

The dolomite sampled for this study occurs as sharply defined, light brown lenses and irregular pods, in the white Madison limestones. The lenses vary in thickness from one to eighteen inches and are three to thirty feet long. One sampled lens was laterally extensive for 100+ yards. The irregular pods range in size from three to ten inches wide and sixteen to forty inches long.

Dolomitization Models

Dolomite is a common, widely occurring sedimentary rock-forming mineral, particularly in the late Precambrian and Paleozoic. In the Mesozoic, between the Jurassic and Cretaceous the amount of dolomite compared to limestone in the rock record decreases, becoming relatively rare in the Holocene (Given and Wilkinson, 1987).

Penecontemporaneous Holocene dolomites were discovered in the late 1950's and early 1960's in intertidal to supertidal marine environments. Dolomite forming in these marginal environments suggested the Mg/Ca molar ratio needed for dolomitization was greater than

the seawater ratio of approximately five. Subsequent research led to the development of numerous dolomitization models to explain dolomite forming in these environments. These models, summarized below, concentrated on Mg/Ca ratios needed for dolomitization and on Mg supply. For a summary of published models and chemistries needed for dolomitization see Morrow (1982a, 1982b), Land (1985) and Hardy (1987).

The Hypersaline Lagoon and Reflux Model was one of the first models proposed for large scale dolomitization (King, 1947; Adams and Rhodes, 1960). In this model, an open marine seawater moves landward across a hypersaline lagoon. Evaporation occurs, resulting in waters with increased density. These evaporated, high density waters infiltrate underlying sediment and move seaward through seaward dipping beds by seepage reflux, causing dolomitization in the process. Mg^{+2} is continually supplied for dolomitization by replenishment of open marine waters to the hypersaline lagoon and subsequent transport of the resultant brines by seepage reflux seaward through the underlying sediment. The Hypersaline Lagoon and Reflux Model has been applied to modern examples by Deffeyes, et al. (1965) and Murray (1969) at Bonaire, Netherlands Antilles, by Muller and Teitz (1971) in the Canary Islands, Kocurko (1979) at San Andres Island and Pierre, et al. (1984) in the Gulf of California.

The Coorong Model arose from work by Alderman and Skinner (1957) on the Coorong Lagoon and a series of ephemeral lakes that extend along the south coast of Australia. In this system, the Coorong Lagoon fills with seawater and the ephemeral lakes fill with groundwater during the humid winter months and evaporate partially or completely during the summer. Calcite and aragonite dominate in the lagoon with dolomite precipitation occurring in the ephemeral lakes. The source of Mg^{+2} for the dolomite is either seawater or the groundwater which may get Mg^{+2} from the weathering of basic volcanic rocks (Van

der Borch, et al., 1975). In either case, Mg^{+2} is supplied for dolomitization by circulation through groundwater flow. The Coorong Model can be thought of as a specialized case of the mixing model, and has been applied to many ancient sequences in which aphanitic dolomite is present and not associated with evaporites (Van der Borch, et al., 1975; Van der Borch, 1976; Van der Borch and Lock, 1979; Muir et al., 1980; Rosen, et al., 1988).

The Sabkha Model was proposed by Illing, et al. (1965), after completion of an extensive study of Holocene sediments exposed on a sabkha near the Qatar Peninsula in the Persian Gulf, in which intertidal and supratidal dolomite had replaced aragonitic sediments. The dolomites in sabkha environments are accompanied by evaporites. Distribution of dolomite in sabkhas along the Persian Gulf are strongly controlled by flood channels across the sabkha. Flood tides are driven landward by storms, reaching maximum penetration along these channels (Patterson, 1972). Moving landward across the sabkha, the frequency of flooding decreases. This is accompanied by a gradual increase in the Mg/Ca ratio and salinity of the floodwaters landward, due to evaporation and gypsum precipitation. The dense Mg^{+2} rich floodwater brines sink into the underlying sediment and flow seaward by seepage reflux, causing dolomitization.

An alternative model to seepage refluxation for Mg^{+2} supply and flow in the sabkha environment is the evaporitic pumping model. In this model, seawater moves landward through sediments underlying the sabkha to replace groundwater lost at the sabkha surface to evaporation, causing dolomitization. Mg^{+2} for dolomitization is continually supplied by this seawater moving landward. The evaporative pumping model has been applied by Hsu and Siegenthaler (1969), Hsu and Schneider (1973) and MacKenzie, et al. (1980). The initial study of Illing, et al. (1965) on sabkha dolomitization was followed by studies of sabkhas at Abu Dahbi, UAE, by Kinsman (1966), Butler (1969), Patterson (1972), de

Groot (1973), Bush (1973), Hsu and Schneider (1973) and Patterson and Kinsman (1981,1982).

The mixed water or dilution model arose from the work of Hansaw, et al. (1971) on the deep confined Tertiary aquifer of Florida. This study was the first to demonstrate that fresh groundwater could influence large-scale dolomitization. In this model, marine derived Mg^{+2} is supplied for dolomitization by continuously circulating groundwater. In work on Middle Pleistocene reef rock of Jamaica, Land (1973) argued from field, petrographic, and chemical data that dolomitization occurred penecontemporaneously by the interaction of fresh groundwater with marine groundwater in a shallow coastal aquifer. Land also suggested many ancient platform dolomites, which are depleted in Na^{+} and trace elements like Sr^{+2} , heavy isotopes like ^{18}O and ^{13}C and lack associated evaporites, may have similarly formed. Folk Land (1975) and Morrow (1982a) argued the dilution of saline solutions by fresh groundwater will cause slow mineral precipitation, which favors the formation of dolomite, because it will allow Ca and Mg ordering in the crystal lattice. High CO_3^{-2} concentrations in many dilute groundwaters may also favor dolomitization in a mixed water setting (Lippman, 1973; Morrow, 1982a). The mixed water or dilution model was applied to other ancient deposits by Badiozamani (1973), Land, et al. (1975), Randozzo and Hickey (1977), Dunham and Olson (1980) and Choquette and Steinen (1980).

The Burial Compaction Model was proposed initially by Illing (1959). In this model, compaction of fine-grained sediments during burial results in the progressive expulsion of Mg^{+2} bearing pore waters which pass through adjacent limestones and cause dolomitization. Mg^{+2} released during the diagenesis of clays and associated amorphous material and ions released during the maturation of organic matter have been considered

additional sources of Mg^{+2} . Early supporters of this model included Griffin (1965) and Jodry (1969). Advances in the understanding of clay diagenesis and associated minerals and in the parallel maturation of organic matter led to renewed consideration of this model (Davies, 1979; Mattes and Mountjoy, 1980).

The Solution Cannibalization Model was proposed by Goodell and Garman (1969). Mg^{+2} for dolomitization is supplied by the dissolution of high-magnesian calcite and reprecipitation of low-magnesian calcite. Kendall (1977) applied this model to the dolomitization of burrow fillings. Recently, the Solution Cannibalization Model has been applied to the phenomena of pressure solution dolomitization (Wanless, 1979). Here, Mg^{+2} for dolomitization derives from the pressure solution of pre-existing magnesian calcite or dolomite. The Solution Cannibalization Model, however, has limited application because other Mg^{+2} sources are required for extensive dolomitization (Hsu, 1966).

The Tectonic or Hydrothermal Dolomitization Model has been applied to dolomites that exhibit cross cutting relationships with enclosing strata. Mg^{+2} is supplied by subsurface brines with high Mg:Ca ratios. The brines move along faults and other zones of high permeability which results in dolomites exhibiting cross cutting relationships with the enclosing strata. This model for dolomitization has been applied by Zenger (1976), Beales and Hardy (1980), Gregg (1985) and Gregg and Hagui (1987).

The discovery of significant amounts of dolomite in modern, organic-rich marine sediments at Deep Sea Drill Project sites, in the Gulf of California, the Japan Trench, the Peru shelf, the Cariaco Basin and the California borderlands lead to the development of the Sulfate/Organic-rich Dolomitization Model. The association of dolomite with organic-rich sediments has long been known from field observations (e.g. Bramlette, 1946). More intimate relationships of dolomite "floating" in organic matter and particles of organic

matter acting as nuclei for dolomite crystals were noted by Spotts and Silverman (1966). Observations of dolomite in organic-rich sediments from the Deep Sea Drilling Project in the early to late 1970's resulted in a new push of research addressing the role of organic matter in dolomitization. Experimental work in the late 1970's and early 1980's suggested low sulfate (SO_4^{-2}) ion concentrations were essential to dolomitization because SO_4^{-2} acted to inhibit the dolomitization process (Baker and Kastner, 1981). This led to the "Low Sulfate" model proposed by Baker and Kastner (1981).

Laboratory experiments of Baker and Kastner found SO_4^{-2} inhibited dolomitization, although no mechanism for inhibition was proposed and they suggested two scenarios for depleting SO_4^{-2} concentrations. The most effective method was the reduction of SO_4^{-2} to sulfide (H_2S) by sulfate reducing bacteria in organic-rich sediments. The other method was to lower SO_4^{-2} concentrations by dilution of seawater with large amounts of fresh water. This promoted dolomitization by decreasing concentrations of the SO_4^{-2} inhibitor. Baker and Kastner preferred the bacterial SO_4^{-2} reduction method because it promoted dolomitization in three ways: (a) by removal of the SO_4^{-2} inhibitor, (b) by increasing alkalinity and (c) by production of NH_4^+ which exchanged for adsorbed Mg^{+2} making Mg^{+2} available for dolomitization. The Low Sulfate Model proposed has been applied primarily to Quaternary and Tertiary "organic" dolomites that exhibit light and heavy carbon isotopic signatures (e.g. Kelts and McKenzie, 1982; Guanatilaka, et al., 1984; various papers in Garrison, et al., 1984; Baker and Burns, 1985). Compton (1988) further showed that the degree of supersaturation of dolomite in the sulfate reducing zone at Deep Sea Drilling Project sites ranged from 4 to 1950 times supersaturated with most waters falling between 60 and 250 times supersaturated. The zone of sulfate minimum and alkalinity maximum, where dolomite supersaturation is usually greatest, occurs from less

than one meter below the sediment/water interface to tens of meters below the interface. Patterson and Kinsman (1982) and Shimmield and Price (1984) noted in research on dolomitization in the Arabian Persian Gulf and Baja California, respectively, that dolomite did not occur in the sediment column until after reducing conditions had been achieved. The depth of sulfate minimum/alkalinity maximum depends in part on the sedimentation rate, organic input and rate of sulfate reduction (Compton, 1988).

Significance of Carbon Isotope Values for Dolomite

Numerous interpretations of depth-related zones for the origin of diagenetic dolomite and authigenic carbonates are based upon carbon isotope values. Isotopic values for organogenic dolomites range from -15‰ to $+20\text{‰}$ PDB (Spotts and Silverman, 1966; Aharon, et al., 1977; Hein, et al., 1979; Friedman and Murata, 1979; Irwin, 1980; Pisciotta and Mahoney, 1981; various papers from Garrison et al., 1984; Burns and Baker, 1987; Sweeny, et al., 1987; Machemer and Hutcheon, 1988). The carbon isotopic composition of carbonates originating in organic-rich sediments depends on the amount of carbonate (CO_3^{2-}) derived from the different zones of bacterial organic matter decomposition (sulfate reduction, methanogenesis, fermentation and eventually thermal degradation) relative to the amounts of CO_3^{2-} derived from seawater bicarbonate (HCO_3^-) and the precursor calcite and aragonite (Claypool and Kaplan, 1974). Very negative carbon isotopic values are interpreted to represent carbonate precipitation in the zone of sulfate reduction. Sulfate reducing bacteria preferentially metabolize lactate and pyruvate with isotopically light carbon resulting in the production of isotopically light CO_2 and thus, CO_3^{2-} . The light CO_3^{2-} is subsequently incorporated into carbonates precipitating in this zone. Very positive carbon values have been interpreted to indicate carbonate precipitation

in the zone of methanogenesis (e.g. Kelts and McKenzie, 1984). During methanogenesis, isotopically light CO_2 is metabolized by bacteria resulting in the production of isotopically light methane (-60‰ to -80‰ PDB) leaving an isotopically heavy CO_2 residual. The heavy CO_2 residual is then incorporated into carbonates precipitating in this zone as CO_3^{2-} giving the carbonates a heavy carbon isotopic signature.

Chemical Conditions needed for Dolomitization and Significance of NH_3

Reviewing current models for dolomitization and lines of evidence used to interpret environments of formation for dolomite, one notes Mg/Ca ratio, salinity, alkalinity, presence of sulfate, organic matter and carbon and oxygen isotopic values have been addressed as important factors needed for dolomitization or important indicators of environment of dolomitization. However, if one looks at Deep Sea Drilling Project pore water analysis of sediments rich in organic matter and dolomite or analysis of Eocene Green River Formation and Miocene Monterey Formation samples, considerable amounts of NH_3 and NH_4^+ are present in the diagenetic system (Gieskes, 1973; Presely, et al., 1973; Moore and Gieskes, 1980; Gieskes, et al., 1981; Baker and Kastner, 1981; Simonet and Bode, 1982; Gieskse et al., 1982; Cooper and Evans, 1983; Slaughter and Mathews, 1984; Gieskse, et al., 1984; various papers from Garrison, et al., 1984). Baker and Kastner (1981) and others (various authors in Garrison, et al., 1984) suggested NH_4^+ was important in diagenesis because NH_4^+ would exchange for adsorbed Mg^{+2} on amorphous silicates, thus providing Mg^{+2} for dolomitization. Slaughter and Mathews (1984) in work on the Eocene Green River Formation, suggested a more intimate role for NH_3 in dolomitization. They proposed NH_3 is important in diagenesis and dolomitization because it is the only natural base produced in significant enough quantities to raise the pH of a

system high enough to allow carbonate precipitation. Geblein, et al., (1973) noted an intimate relationship between lithified algal material and dolomite. Dolomite was concentrated in the algal rich sediments. Algae is dominantly protein, which will produce abundant NH_3 when decomposing in a reducing environment.

MADISON FORMATION CASE STUDY

Sampling

Thirteen samples of the dolomite pods and associated limestones in the Madison Formation near Lander, Wyoming were collected between June, 1987 and October, 1987 at various locations within the stratigraphic section (see Figure 1). Each sample was stored in plastic bags during preparation and analysis. Each sample described by numbers 1 through 13 below, contained a limestone and a dolomite sample. Samples 1, 2, 3, and 6 were collected in the Shoshone National Forest near the VABM in Limestone Mountain on the Miner's Delight 7.5 minute quadrangle topographic map. This area was not divided into 1/4 sections. Samples 4 and 5 were collected in NW1/4SE1/4SW1/4 of section 9 of the Miner's Delight quadrangle. Samples 7 and 8 were collected in the NW1/4NW1/4 NW1/4 of section 9 of the Miner's Delight quadrangle and sample 9 was collected in the SE1/4SE1/4SE1/4 of section 4 of the Miner's Delight quadrangle. Samples 10, 11 and 12 were collected in the NW1/4NW1/4NW1/4 of section 20 of the Fossil Hill 7.5 minute quadrangle topographic map and sample 13 was collected in the SE1/4NE1/4NE1/4 of section 19 of the same map. A hand specimen of limestone and dolomite from each sampling location was collected for macroscopic and thin section analysis.

Dolomite pods were located by following Madison outcrops, and the pods were sampled as each was discovered. The dolomite pods had not been previously mapped by other researchers. Enough rock (5 to 10 pounds) was collected in each sample so that separation of the less than 2 micron fraction would produce enough clay for x-ray diffraction analysis and trace nitrogen analysis. After collection, the samples were brought to the Colorado School of Mines for preparation and analysis.

Table 1. Sample location of limestone/dolomite pairs from Madison Formation, Wyoming

Sample	7.5 minute quadrangle	Section	Quarter section
1*	Miner's Delight	Shoshone National Forest	near VABM
2*	Miner's Delight	Shoshone National Forest	same as above
3*	Miner's Delight	Shoshone National Forest	same as above
4	Miner's Delight	9	NW ¹ / ₄ SE ¹ / ₄ SW ¹ / ₄
5	Miner's Delight	9	NW ¹ / ₄ SE ¹ / ₄ SW ¹ / ₄
6*	Miner's Delight	Shoshone National Forest	near VABM
7	Miner's Delight	9	NW ¹ / ₄ NW ¹ / ₄ NW ¹ / ₄
8	Miner's Delight	9	NW ¹ / ₄ NW ¹ / ₄ NW ¹ / ₄
9	Miner's Delight	4	SE ¹ / ₄ SE ¹ / ₄ SE ¹ / ₄
10	Fossil Hill	20	NW ¹ / ₄ NW ¹ / ₄ NW ¹ / ₄
11	Fossil Hill	20	NW ¹ / ₄ NW ¹ / ₄ NW ¹ / ₄
12	Fossil Hill	20	NW ¹ / ₄ NW ¹ / ₄ NW ¹ / ₄
13	Fossil Hill	19	SE ¹ / ₄ NE ¹ / ₄ NE ¹ / ₄

* no quarter section

Sample Preparation

All samples were crushed to approximately 1/4 to 1/2 inch diameter particles using a jaw crusher. Before crushing, each sample was cleaned with a wire brush to remove surface contamination. Between crushing of each sample, the jaw crusher was cleaned with a wire brush and compressed air and then "contaminated" with a portion of the subsequent limestone or dolomite to be crushed. This was done to minimize contamination from previous use of the jaw crusher. All limestone samples were crushed consecutively in random order to minimize contamination between limestone and dolomite samples. All limestones were crushed before crushing the dolomites to eliminate contamination from the dolomite, which may have contained ammonium clays, making the nitrogen analysis less significant. The same procedures were followed for the dolomite samples.

Grinding the samples to 1/32 to 1/64 inch diameter particles using a ceramic plate grinder followed crushing. A ceramic plate grinder was prepared for use, using methods similar to preparation of the jaw crusher.

To ensure that splits of each sample for chemical and mineralogical analysis were representative, each sample was homogenized in a roller mill for seven days. The samples were mixed by hand once each day to eliminate grain segregation due to grain size differences that may have arisen during rolling. Mixing was done in plastic chemical bottles. The bottles were cleaned with soap and water, rinsed with water and then rinsed with methyl alcohol for quick drying. Before using the bottles for subsequent samples, the bottles were vigorously (by shaking) rinsed three times with water and then with methyl alcohol.

Once homogenization was complete, each sample was split into four equal portions using a sample splitter. One split was used for separation of the less than 2 micron fraction

Figure 1 Madison Formation Section
near Lander, Wyoming

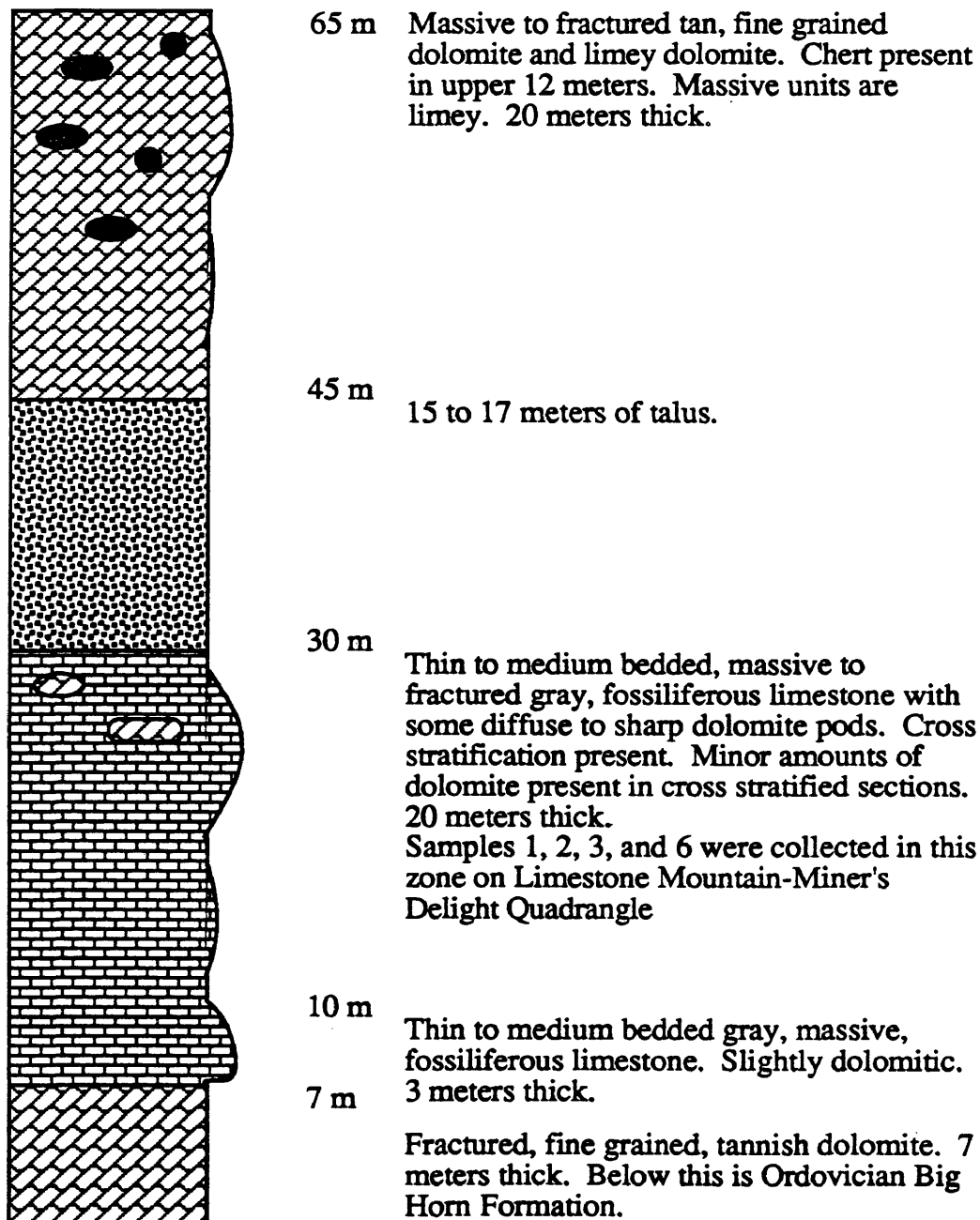
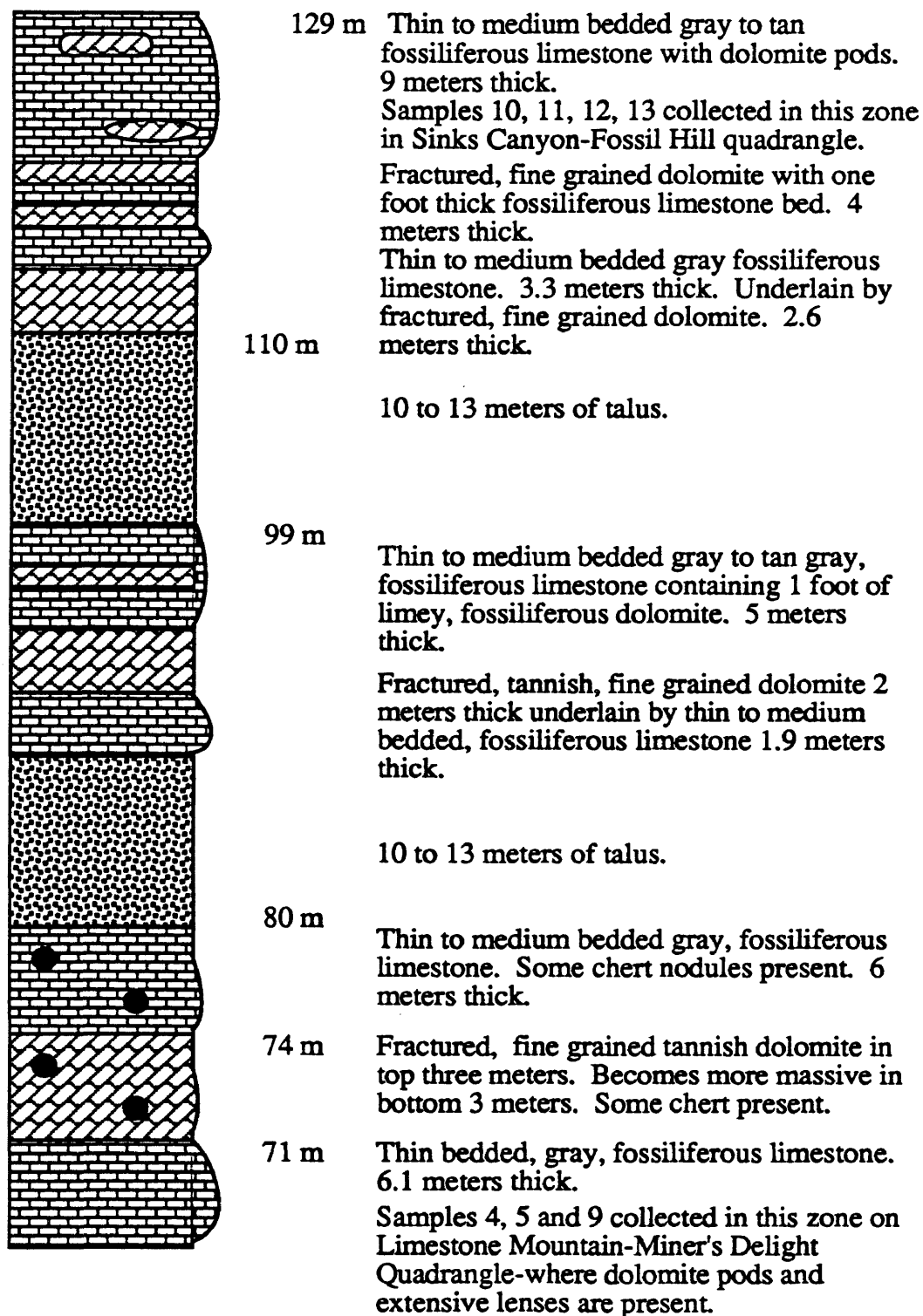


Figure 1 continued



for x-ray analysis of clays and trace nitrogen analysis. Portions of the second split were used for bulk mineral identification by x-ray diffraction, bulk chemical analysis by x-ray fluorescence and mineral CO₂ and H₂O analysis. The third and fourth splits were extra. The splitter and splitting trays were cleaned by first brushing the dust out, and then rinsing with methyl alcohol for quick drying and to prevent corrosion. The splitter and trays were wiped again after drying to eliminate dust and minimize contamination between samples.

Gravity separations to obtain the less than 2 micron fraction were done in 1000 ml graduated cylinders. Approximately 300 ml of deionized water was added to the graduated cylinder. Then a portion of one sample split was added with more deionized water to 1000 ml total volume. Approximately one-third gram of sodium hexa-metaphosphate was added to each graduated cylinder to prevent flocculation of the clays. The samples were then stirred and allowed to settle for eight hours and ten minutes. At the end of this time period, the top ten centimeters of liquid was siphoned from each cylinder and collected in a separation vessel. This liquid was centrifuged to force sedimentation of the less than 2 micron fraction. The separation and centrifugation process was repeated until approximately 2-3 grams (dry weight) of solid were collected. The less than 2 micron fraction was dried in an oven at 100°C and homogenized for five days on a tube rotator to ensure obtaining a representative sample for x-ray diffraction and trace nitrogen analysis.

The less than 2 micron fraction contained greater than 90% carbonate minerals, which did not allow for identification of the clays due to the small percentage of clays in the samples and dilution by the carbonate minerals. The separation procedure was repeated for the less than 1 micron fraction using approximately 100 grams of sediment and 1 gram of sodium hexametaphosphate. Centrifuging was done with a Sharples super centrifuge at 25,000 r.p.m. The samples were washed with distilled water during centrifugation to

eliminated sodium hexa-metaphosphate. The sediment was further segregated according to grain size during centrifugation. The finer material, which accumulates near the top of the centrifuge tube, was preferentially used for x-ray diffraction analysis, to insure less dilution by fine carbonates. This method produced interpretable x-ray diffraction patterns.

Quantitative Mineral Analysis

Quantitative mineral amounts and mineral compositions were determined using QMAS, a computer program which combines mineralogy from x-ray diffraction, bulk chemistry from x-ray fluorescence, mineral CO₂ analysis, H₂O+, H₂O-, and mineral nitrogen and Fe⁺² analysis. Mineral amounts and compositions are solved using linear programming techniques. The theory of QMAS is summarized in Appendix B.

X-Ray Diffraction Analysis

X-Ray diffraction was done by standard methods. The bulk mineralogy of each sample was determined by analysis of a random, front-loaded bulk mount. A one micron Al₂O₃ internal standard was mixed into each bulk sample for 48 hours at a ratio of 1.200 grams of sample to .300 grams of Al₂O₃. Mineral amounts were estimated by comparing integrated intensities. The bulk samples were run on a Philips diffractometer at 36 KV, 15ma, 500 cps full range, 128 amplifier gain and 1 degree 2 theta per minute scan rate.

The less than one micron clay mineralogy for each sample was determined by analysis of an oriented smear mount on a glass slide. The clay fractions were glycolated for one hour at 80° C to expand all smectite minerals before analysis. The clay mounts were subsequently heated for two hours at 600° C and x-rayed to detect iron-rich chlorite. The

clay fractions were run at 40 KV, 20 ma, 500 cps full range, 128 amplifier gain and 1 degree 2-theta per minute scan rate from 2 to 35 degrees 2-theta.

Bulk Chemical Analysis

Bulk chemical analysis was done by x-ray fluorescence methods using a fused pellet containing 1.25 grams of sample. The elements analysed were Si, Al, Fe, Ti, Ca, Mg, Na, K, S, and P. Matrix corrections were made by a modified version of CORSET (Stevenson, 1971). Samples were prepared for x-ray fluorescence analysis by high temperature ashing the sample at 850° C, mixing with lithium tetraborate for two days and then fusing with a Claisse automatic fuser. A standard similar to the unknowns were used during the analysis by a Philips 1400 series automated x-ray spectrometer. FeO was determined by the U.S.G.S. method with an analytical sensitivity of .02 percent.

CO₂ and H₂O Analysis

CO₂ analysis was done by placing the sample in a tube combustion furnace controlled by a PID controller which releases mineral and organic CO₂ from the sample. The analyte gases are carried, using oxygen as the carrier gas, through heated tubing to a catalytic oxidizer to oxidize the remaining organic matter, through a one micron dust filter and into the detector. The detector is a Luft-type infrared analyser. The process is controlled by an IBM/AT or compatible computer. The IBM/AT logs the data and computes the results. A non-linear least squares curve fitting program differentiates different curves produced by the analyser. Each curve represents a different source of CO₂. Total organic carbon, organic CO₂ and carbonate CO₂ are differentiated with different carbonate fractions determined when possible.

Water expelled by heating a sample at 105-110° C is designated surface water (H₂O-) and water expelled above 110° C is designated structural water (H₂O+). The amount of water lost is determined by weighing after the sample has cooled in a dessicator.

Chemical Analysis Problems Associated with QMAS

Structural water presents the most significant problem in quantitatively determining the amount of clay minerals in a sample. Clay minerals and zeolites release an unspecified amount of interlayer and cation bound water well above 110° C and allophane loses hydroxyl (OH⁻) water on static heating down to 100° C.

The important water for determining mineral amounts is hydroxyl water for samples in this study. When the hydroxyl bearing minerals comprise muscovite, well crystallized kaolinite and metamorphic chlorites, the conventional analysis of hydroxyl water is sufficiently accurate to ensure good analysis. If, however, halloysite or allophane, illite, smectites and zeolites are rock components, the errors in structural water content can introduce large errors in mineral quantities. For almost all rocks containing nondiscriminant water, the amount of structural water must be adjusted manually or treated as a variable with structural water added or subtracted from the total water analysis. Corresponding decreases or increases in unbound water also occur until the objective function is maximized. Adjusting the structural water content to maximize the objective function effectively introduces a third linear programming problem. QMAS does this adjustment internally.

The determination of sulfide or non-sulfate sulfur is difficult, because it is hard to maintain an oxidizing environment throughout all stages of sample preparation of organic-rich sediments. Incomplete oxidation of sulfide sulfur as SO₂ results in low S values and

causes excess Fe^{+2} in the analysis to be allocated to illites, chlorites and smectites, both as Fe^{+2} and Fe^{+3} , giving erroneous clay compositions. Accurate determination of CO_2 , which is usually underestimated by standard methods, is also important for the same reason.

Mineral Nitrogen Analysis

Mineral nitrogen analysis was done at Huffman Laboratories in Golden, Colorado, using the Carlo Erba (modified Dumas) method. Approximately 100 micrograms of sample is placed in a tin capsule and heated to 1000°C in the presence of oxygen gas. At 1000°C the tin capsule and sample combust, raising the temperature in the sample chamber to approximately 1600°C . Nitrogen in the sample oxidizes to nitrous oxide. A helium purge sweeps the gases created by combustion of the sample through the combustion tube and to a scrubber, which removes water produced during the combustion. Scrubbers can also be installed to remove CO_2 if desired. After the scrubbers, the gases pass through a copper tube where excess oxygen is removed and nitrous oxides reduced to nitrogen gas. From the copper tube the gases go to a carbon/nitrogen detector which detects the nitrogen gas. Results are then expressed in parts per million of N.

Strontium Isotope Analysis

Two dolomite samples (3 and 10) were analysed for $^{87}\text{Sr}/^{86}\text{Sr}$ ratios at CU-Boulder. The samples were dissolved in hydrochloric acid and then separated by ion exchange. Isotope ratios were determined by comparison with standard SrCO_3 (NBS SRM987) which has an assumed value .71014. The 85, 86, 87, and 88 masses were collected in four separate faraday cups. The $^{87}\text{Sr}/^{86}\text{Sr}$ values were corrected for the presence of ^{87}Rb and

normalized to $^{86}\text{Sr}/^{88}\text{Sr} = .1194$ with a precision of $\pm .00005$ at the 95% confidence level.

Carbon Isotope Analysis

Limestone and dolomite carbon isotope values were determined by reacting the sample with 100% phosphoric acid at 25° C and 50° C, respectively. The reaction was done in glass reaction tubes sealed under vacuum. Between 15 and 20 micrograms of sample was reacted and the liberated CO₂ was collected in glass tubes and sealed under vacuum. The CO₂ was analysed on a Varian MAT 250 mass spectrometer, relative to the Cretaceous Peedee Formation Belemnite standard.

Thin Section Analysis

Thin sections of each limestone and dolomite sample collected were cut and stained using alizarin red to differentiate calcite from dolomite. Rocks in thin section were classified according to Folk's classification (Folk, 1959) and Dunham's classification (Dunham, 1962). Dolomites were classified also according to Sibley and Gregg classification (Sibley and Gregg, 1987). Analysis of grain type and diversity was emphasized for the limestones. Analysis of grain preservation and texture was emphasized for the dolomites. Presence and texture of accessory minerals were also noted to help determine clastic or authigenic origin.

Cathodoluminescence

Cathodoluminescence was performed on the dolomite samples at the University of Colorado at Boulder with the assistance of Dr. David Budd. This method is used to

determine compositional variations in minerals qualitatively. It is particularly useful for looking at iron and manganese variations in carbonates and mineral zoning. Manganese causes bright luminescence while iron quenches luminescence.

RESULTS

Bulk Mineralogy and Chemistry of Limestone and Dolomite Samples

The bulk mineralogy of the limestone and dolomite samples are summarized in Tables 2 and 3, respectively. Semiquantitative bulk mineral amounts are expressed as weight percentages of the total sample. Accessory minerals in the Madison Formation are minor constituents. The clay minerals are not expressed in the bulk analysis, because their amounts are too small to allow accurate determination without separation of the less than one micron fraction. The limestones and dolomites of the Madison Formation contain few accessory minerals. Calcite is the dominant mineral in the limestones with minor amounts of dolomite and quartz. Mean albite content of the dolomites is 4 times greater than albite in limestones. Mean microcline content of the dolomites is 7 times greater than albite in limestones. Dolomite is the dominant mineral in the dolomite samples with minor amounts of calcite and quartz. Some detrital quartz and/or feldspar grains were observed in fourteen of twenty four samples in thin section as well rounded, silt sized material. The quartz and/or feldspar grains are described this way, because although some grains have hints of twinning, their fine size precludes distinguishing them from each other. Authigenic quartz is present in thin section.

The bulk whole rock chemistry of limestone and dolomite samples are summarized in Table 4. The bulk chemistry reflects the dominantly carbonate mineralogy and lack of accessory minerals observed in the Madison Formation. Alumina and silica are present in small amounts, consistent with the minor amounts of feldspar and quartz observed. Potassium and iron are minor constituents. Low sulfur content of the limestone and dolomite is a result of the low iron content, which precluded the formation of significant

pyrite during diagenesis. The phosphate content is consistent with high organic productivity during deposition of the Madison Formation.

Table 2. Bulk mineralogy of limestone samples (weight %)*

Sample	dolomite	calcite	siderite	quartz	pyrite	albite	microcline
1	20.9	76.8	0	2.4	0	0	0
2	5.8	88.3	1.8	4.1	0	0	0
3	34.3	60.2	1.0	2.0	0.8	1.1	0.6
4	1.4	93.7	0	4.0	0	0.9	0
5	0	95.1	0	3.9	0	0.9	0
6	3.5	93.1	0	3.3	0	0	0
7	0.7	96.6	0	1.4	0.8	0.5	0
8	6.6	87.2	0	4.3	0	1.2	0.7
9	0.8	96.0	0.8	3.4	0	0	0
10	1.7	96.0	0	2.4	0	0	0
11	0	96.8	0	3.2	0	0	0
12	5.4	86.8	0	3.2	0	1.3	0
13	0.9	95.9	0	2.6	0	0.7	0
Average			0.3	3.0	0.1	0.5	0.1

* Illite was not detected in any bulk samples because of dilution by other minerals

Table 3. Bulk mineralogy of dolomite samples (weight %)*

Sample	dolomite	calcite	siderite	quartz	pyrite	albite	microcline
1	77.7	5.9	0	6.1	0	5.4	4.9
2	88.4	5.9	0	1.8	1.5	2.6	0.7
3	90.6	2.3	1.0	2.3	0.9	2.4	0.4
4	85.9	6.3	0	5.1	0.9	1.8	0
5	81.4	13.1	0	1.3	1.3	2.0	0.7
6	83.1	12.9	0	1.2	1.0	1.8	0
7	81.6	11.1	0	3.0	1.1	2.3	0.8
8	87.7	3.1	0.7	5.5	0.5	1.9	0.4
9	82.7	7.8	0	4.0	1.5	2.2	1.7
10	76.3	13.0	0	5.3	0.7	2.8	1.8
11	81.8	12.3	0	2.0	1.7	2.2	0
12	99.0	5.6	0	1.9	0	1.9	0.6
13	81.7	13.0	0	1.2	1.2	2.0	0.7
average			0.1	1.0	1.0	2.1	0.7

* Illite was not detected in any bulk samples because of dilution by other minerals

Table 4. Whole rock bulk chemistry of selected limestones and dolomites

Sample	1L	1D	4L	4D	5L	5D	9L	9D	10L	10D	12L	12D
SiO ₂	.213	.164	1.14	.537	1.25	.684	.358	.485	1.82	2.20	.661	.846
TiO ₂	.0037	.0025	.0036	.0006	.00	.00	.0031	.0092	.0058	.0194	.0027	.00
Al ₂ O ₃	.474	.467	.360	.288	.310	.276	.312	.405	.383	.542	.351	.250
Fe ₂ O ₃	.0336	.153	.0317	.0585	.00	.191	.0283	.193	.0243	.467	.0266	.0654
CaO	47.03	32.52	45.93	32.30	51.40	33.78	51.64	35.08	50.19	32.93	50.79	33.61
K ₂ O	.0019	.0309	.0058	.0040	.0013	.0021	.0163	.0194	.0321	.0653	.0089	.0007
MgO	7.27	18.96	8.33	20.05	3.33	19.31	3.37	17.70	3.19	17.28	3.65	19.06
Na ₂ O	.0863	.0181	.0811	.0118	.0587	.0164	.0820	.0143	.0660	.0084	.0325	.0180
BaO	.00	.00	.00	.00	.00	.00	.00	.0006	.00	.0006	.00	.00
P ₂ O ₅	.0084	.0123	.0043	.0060	.0010	.0061	.0024	.0164	.0031	.0145	.0029	.0035
SO ₃	.00	.00	.00	.00	.0036	.00	.00	.00	.00	.00	.00	.00
H ₂ O	.0600	.0300	.0600	.0300	.0900	.120	.0600	.0900	.0600	.120	.150	.120
H ₂ O+	.110	.130	.340	.230	.0901	.120	.120	.0901	.130	.150	.110	.130
CO ₂	43.97	47.24	43.01	46.27	43.07	45.28	43.29	45.71	43.45	46.14	43.76	45.74
Org**	.00	.00	.00	.00	.00	.00	.00	.00	.00	.00	.00	.00
Total	99.21	99.70	99.24	99.78	99.52	99.67	99.23	99.73	99.30	99.83	99.40	99.73

+ L-limestone; D-dolomite

* FeO was determined by the U.S.G.S. method. The method has analytical sensitivity of about 0.02%. Thus, any FeO

value

could range from 0 to 0.02.

** Org - organic matter

Mineralogy and chemistry of the Less than one micron fraction for Limestones and Dolomites

The mineralogy of the less than one micron fraction of the limestone and dolomite samples are summarized in Table 5 and Table 6. The chemistry of the less than one micron (clay) fraction is summarized in Table 7. The mineralogy for the less than one micron fractions was determined by QMAS using the chemistry of Table 7 and the mineralogy of the clay fraction as identified from x-ray diffraction. QMAS determines quantitative mineral amounts. The clay fraction contains about 85% carbonate minerals with illite, quartz, hydrous phosphate and amorphous $\text{AlO}(\text{OH})$ dominating the remainder of each sample.

Two important results are observed in the chemistry of the clay fraction. First, potassium is a trace constituent in all samples. Ammonium, which substitutes for potassium in sedimentary minerals, is present in 5 to 85 times greater amounts than potassium in the dolomite clay fraction samples analysed and .75 to 40 times greater in the limestone clay fraction samples analysed. The relationship between potassium and ammonium amounts is summarized in Table 8. Second, the limestone and dolomite samples have extremely low iron content. The low iron content of the clay fraction is consistent with diagenesis in the zone of bacterial sulfate reduction where there is lack of iron bearing minerals in the bulk mineralogy. The distribution of iron within the minerals is consistent with mineral formation in the sulfate reducing and methanogenic zones.

Carbon Isotopes

The carbon isotope values relative to PDB standard for selected limestone and dolomite samples are summarized Table 9. The limestone and dolomite carbon isotope values are near zero, which are slightly lighter than the estimated value for Mississippian

Table 5. Mineralogy of limestone less than one micron fractions from QMAS analysis

Sample	Mineral	Weight Percent	Volume Percent
<i>1 Limestone</i>	Calcite	72.23	73.07
	Dolomite (Fe.003)	22.87	22.08
	Illite-NH ₄ ⁺	1.28	1.50
	Quartz	.15	.16
	Pyrite	.00	.00
	Rutile	.01	.00
	Hydrous Phosphate	1.85	1.85
	AlOOH-amorphous	1.57	1.30
Objective function = 99.96			
Illite NH ₄ ⁺ .77K.07Na.01Mg.05Fe ⁺³ .25Fe ⁺² .02Al _{2.47} Si _{3.21} O ₁₀ ·2H ₂ O			
<i>4 Limestone</i>	Calcite	89.91	90.04
	Dolomite Fe .000	.71	.68
	Illite-NH ₄ ⁺	1.46	1.70
	Quartz	1.79	1.84
	Pyrite	.04	.02
	Rutile	.00	.00
	Hydrous Phosphate	4.23	4.19
	AlOOH-Amorphous	1.82	1.49
Objective function = 99.959			
Illite NH ₄ ⁺ .80K.02Na.02Mg.03Fe ⁺³ .07Fe ⁺² .04Al _{2.66} Si _{3.21} O ₁₀ ·2H ₂ O			
<i>5 Limestone</i>	Calcite Mg .006	86.74	86.68
	Dolomite Fe .010	.35	.34
	Illite-NH ₄ ⁺	3.38	3.90
	Quartz	.95	.97
	Pyrite	.01	.00
	Rutile	.03	.02
	Hydrous Phosphate	6.39	6.32
	AlOOH-Amorphous	2.10	1.71
Objective function = 99.951			
Illite NH ₄ ⁺ .54K.23Na.00Mg.03Fe ⁺³ .43Fe ⁺² .01Al _{2.27} Si _{3.26} O ₁₀ ·2H ₂ O			
<i>9 Limestone</i>	Calcite Mg .009	92.32	92.53
	Dolomite Fe .003	.26	.24
	Illite-NH ₄ ⁺	1.13	1.31
	Quartz	2.66	2.74
	Pyrite	.01	.00
	Rutile	.03	.02
	Hydrous Phosphate	1.18	1.17
	AlOOH-Amorphous	2.40	1.96
Objective function = 99.979			
Illite NH ₄ ⁺ .41K.54Na.01Mg.05Fe ⁺³ .34Fe ⁺² .10Al _{2.36} Si _{3.15} O ₁₀ ·2H ₂ O			
<i>10 Limestone</i>	Calcite Mg .020	93.73	93.71
	Dolomite Fe .003	.30	.29
	Illite-NH ₄ ⁺	1.25	1.44
	Quartz	1.89	1.94
	Pyrite	.00	.00
	Rutile	.01	.00
	Hydrous Phosphate	1.81	1.79
	AlOOH-Amorphous	.98	.80
Objective function = 99.978			
Illite NH ₄ ⁺ .53K.25Na.01Mg.03Fe ⁺³ .30Fe ⁺² .03Al _{2.39} Si _{3.25} O ₁₀ ·2H ₂ O			

Table 6. Mineralogy of dolomite less than one micron fractions from QMAS analysis

Sample	Mineralogy	Weight Percent	Volume Percent
<i>1 Dolomite</i>	Calcite	11.08	11.53
	Dolomite	84.65	84.05
	Illite-NH ₄ ⁺	1.15	1.38
	Quartz	.15	.16
	Pyrite	.00	.00
	Rutile	.01	.00
	Hydrous Phosphate	2.00	2.06
	AlOOH-Amorphous	.91	.77
Objective function = 99.996			
Illite NH ₄ ⁺ .67K.13Na.01Mg.05Fe ⁺³ .32Fe ⁺² .03Al _{2.34} Si _{3.25} O ₁₀ ·2H ₂ O			
<i>4 Dolomite</i>	Calcite	9.04	9.36
	Dolomite Fe .006	83.09	82.14
	Illite-NH ₄ ⁺	2.55	3.06
	Quartz	.11	.12
	Pyrite	.00	.00
	Rutile	.00	.00
	Hydrous Phosphate	5.10	5.23
	AlOOH-amorphous	.00	.00
Objective function = 99.909			
Illite NH ₄ ⁺ .84K.01Na.00Mg.04Fe ⁺³ .19Fe ⁺² .05Al _{2.50} Si _{3.22} O ₁₀ ·2H ₂ O			
<i>5 Dolomite</i>	Calcite	17.69	18.30
	Dolomite Fe .010	73.10	72.16
	Siderite	.27	.20
	Illite-NH ₄ ⁺	3.09	3.70
	Quartz	1.12	1.19
	Pyrite	.01	.00
	Rutile	.06	.04
	Hydrous Phosphate	2.58	2.64
AlOOH-Amorphous	1.98	1.67	
Objective function = 99.910			
Illite NH ₄ ⁺ .43K.41Na.00Mg.03Fe ⁺³ .28Fe ⁺² .02Al _{2.47} Si _{3.19} O ₁₀ ·2H ₂ O			
<i>9 Dolomite</i>	Calcite	3.97	4.15
	Dolomite	94.03	93.72
	Illite-NH ₄ ⁺	.87	1.05
	Quartz	.51	.55
	Pyrite	.00	.00
	Rutile	.00	.00
	Hydrous Phosphate	.00	.00
	AlOOH-Amorphous	.57	.49
Objective function = 99.969			
Illite NH ₄ ⁺ .81K.03Na.02Mg.05Fe ⁺³ .19Fe ⁺² .02Al _{2.55} Si _{3.19} O ₁₀ ·2H ₂ O			
<i>10 Dolomite</i>	Calcite	7.54	7.84
	Dolomite Fe .003	86.15	85.57
	Illite-NH ₄ ⁺	1.12	1.34
	Quartz	.43	.46
	Pyrite	.00	.00
	Rutile	.00	.00
	Hydrous Phosphate	4.0	4.17
	AlOOH-Amorphous	.67	.57
Objective Function = 99.962			
Illite NH ₄ ⁺ .82K.07Na.01Mg.08Fe ⁺³ .18Fe ⁺² .10Al _{2.40} Si _{3.24} O ₁₀ ·2H ₂ O			

Table 7. Bulk chemistry of the less than one micron fractions

Sample	1L	1D	4L	4D	5L	5D	9L	9D	10L	10D
SiO ₂	0.792	0.762	2.53	1.37	2.62	2.64	3.18	0.948	2.51	0.996
TiO ₂	0.0123	0.0128	0.0063	0.0061	0.0300	0.584	0.0324	0.0007	0.0109	0.0052
Al ₂ O ₃	1.58	1.02	1.86	0.879	2.55	2.45	2.11	0.718	1.12	0.844
Fe ₂ O ₃	0.0658	0.0756	0.0223	0.106	0.299	0.177	0.0777	0.0338	0.0766	0.0405
FeO*	0.0403	0.172	0.0101	0.213	0.0402	0.465	0.0201	0.0503	0.0201	0.121
FeS ₂	0.0062	0.0091	0.0375	0.0090	0.0103	0.0139	0.103	0.0061	0.0084	0.0099
CaO	48.28	33.20	52.25	32.84	51.15	33.52	51.82	31.27	52.46	32.47
K ₂ O	0.0115	0.0187	0.0042	0.0043	0.0947	0.151	0.0728	0.0035	0.0384	0.0099
MgO	4.89	17.99	0.174	17.64	0.296	15.59	0.395	20.05	0.828	18.35
Na ₂ O	0.0011	0.0014	0.0021	0.0007	0.0014	0.0012	0.0012	0.0015	0.0011	0.0010
BaO	0.0015	0.0017	0.0021	0.0019	0.0026	0.0055	0.0021	0.00	0.00	0.0010
P ₂ O ₃	0.964	1.04	2.20	2.66	3.34	0.135	0.614	0.0044	0.943	0.211
SO ₃	0.00	0.00	0.00	0.00	0.00	0.00	0.00	0.00	0.00	0.00
(NH ₄) ₂ O	0.0854	0.0669	0.104	0.195	0.156	0.115	0.0390	0.0613	0.0576	0.0799
H ₂ O-	0.710	1.00	0.730	1.44	0.570	1.18	0.590	0.570	0.710	1.00
H ₂ O+	0.594	0.424	0.826	0.477	1.13	0.830	0.754	0.191	0.433	0.495
CO ₂	42.68	45.22	39.91	43.61	38.41	42.65	40.80	46.58	41.51	44.37
Org**	0.00	0.00	0.00	0.00	0.00	0.00	0.00	0.00	0.00	0.00
Total	100.0	99.98	99.95	100.05	100.12	100.01	99.93	99.92	100.01	99.90

+ L-limestone; D-dolomite

* FeO was determined by the U.S.G.S. method. The method has analytical sensitivity of about 0.02%. Thus, any FeO value could range from 0 to 0.02.

** Org - organic matter

Table 8. Mineral nitrogen values and NH_4^+ to K^+ ratios for less than one micron fractions

Sample	Limestone		Dolomite	
	NH_4^+ (mol/g $\times 10^{-2}$)	NH_4^+/K^+	NH_4^+ (mol/g $\times 10^{-2}$)	NH_4^+/K^+
1*	2.56	11.00	2.00	5.15
2	1.94	-	2.17	-
3	2.28	-	2.17	-
4	3.11	40.00	5.83	84.00
5*	4.00/4.39	2.35	3.44/3.89	1.05
6	2.61	-	3.06	-
7*	3.06/3.33	-	0.78	1.22
8	0.94	-	1.72	-
9	1.17	0.76	1.83	27.00
10	1.98/2.28	2.12	2.39/2.61	11.71
11	1.17	-	1.94	-
12	1.72	-	2.39	-
13*	5.44	-	3.22	-
2 bulk	<.111	-	0.111	-
13 bulk	-	-	0.333	-

* limestone value higher than dolomite

- data not available

Table 9. Carbon isotope values for some limestones and dolomites*

Sample	Limestone $\delta^{13}\text{C}$ (‰)	Dolomite $\delta^{13}\text{C}$ (‰)
1	NA	1.80
3	NA	1.90
4	0.04	0.07
5	0.98	-0.04
9	1.76/1.71	0.70
10	0.98	1.60
11	0.94	3.00
Mississippian Seawater**	3.9	

* relative to Pee Dee Belemnite standard

** Meyers and Lohman, 1983

NA-not available

seawater (Meyers and Lohman, 1983). Anomalously very positive or very negative carbon isotope values indicating diagenesis in the zone of bacterial sulfate reduction or methanogenesis are not observed, but can be explained.

Strontium Isotopes

Strontium isotope ($^{87}\text{Sr}/^{86}\text{Sr}$) analysis was done on two dolomite samples. Dolomite 3 sample did not contain enough strontium for the amount of sample used to obtain a value. Dolomite 10 yielded a value of .709165 +/- .00005 which corresponds with modern seawater, Cambro-Ordovician seawater (Burke, et al., 1982), and many types of groundwaters. The value for Kinderhookian deposition is approximately .7079 (Popp, et al., 1986).

Thin Section Analysis

In thin section, the limestone samples reveal a diverse fauna consisting of echinoderms, arthropods, corals, brachiopods, foraminifera, molluscs, ooides, pellets and intraclasts. The grains are commonly micritized. The limestones are classified according to Folk as biowackestones, biopackstones and biograinstones (Appendix A). The Madison Formation dolomite replaces fossiliferous limestone. Molds and non-mimically dolomitized fossils are observed. The dolomites are classified as dolomitized equivalents of the limestones. According to the Sibley and Gregg classification the dolomites are unimodal planar-s. The limestones and dolomites are almost non-porous.

The limestone and dolomite samples lack appreciable accessory minerals in thin section. Authigenic quartz filling pore space is the only mineral readily apparent. Careful observation reveals very fine, well rounded, detrital quartz and/or feldspar grains in most thin sections and minor amounts of sulfides.

Cathodoluminescence

Cathodoluminescence was performed on the dolomites of the Madison Formation. The dolomites show dull dolomite cores with some brighter rims of dolomite lining or filling pores. Dull luminescence is usually the result of iron content in the mineral, while bright luminescence indicates manganese.

INTERPRETATION

The Mississippian Madison Formation as sampled, is a clean carbonate unit deposited in a normal marine environment and contains only minor amounts (never more than 15%) of non-carbonate accessory minerals (Tables 1 and 2). Diverse fossil assemblages (Appendix A) confirm that the Madison Formation in the Lander, Wyoming area, was deposited in a normal marine environment with extremely minor detrital input. Some organic matter was initially preserved in the Madison Formation as is indicated by the smell of hydrocarbons at some sampling localities and the presence of NH_4^+ -illite in the clay fraction. The mineralogy observed in the Madison Formation is interpreted to be a direct result of early diagenesis in the zone of bacterial sulfate reduction and probably methanogenesis. In zones where organic matter was preserved, the CO_2 , H_2S and NH_3 , produced during bacterial sulfate reduction and later reduction of CO_2 associated with methanogenesis, controlled pore water chemistry of the Madison Formation, and thus the diagenetic reactions which produced the observed mineral assemblage.

Chemistry and Mineralogy

The chemistry and mineralogy of the Madison Formation are distinctive. The Madison Formation originally contained extremely minor amounts of detrital minerals. The only accessory minerals observed in the bulk mineralogy are albite, microcline and quartz with traces of pyrite and siderite rarely present.. The clay fraction shows NH_4^+ -illite, hydrous phosphate and $\text{AlO}(\text{OH})$ are present in minor amounts. The $\text{AlO}(\text{OH})$ could represent kaolin allophane. These observed mineralogies and mineral compositions are best explained as a product of organic matter degradation in the zone of bacterial sulfate

reduction and methanogenesis. This conclusion is supported by the minor amounts of detrital minerals observed in thin section, the lack of significant accessory minerals in bulk x-ray diffraction patterns and the low iron content of the bulk rocks.

Diagenetic illite is the only clay mineral positively observed in the Madison Formation sediments. The ammonium content of the interlayer cation sites of the illite indicates illite is an authigenic phase that formed in an organic-rich environment during diagenesis. Except for the NH_4^+ and low Mg content, the illites are normal. They have sufficient Fe^{+3} to make the illite stable with respect to microcline and kaolinite or kaolin allophane. The amount of total iron available in the sediment is low due to limited detrital mineral input. Available magnesium, which alternately to Fe^{+3} is necessary in illite octahedral sites, was incorporated into dolomite forming at this time. Some of the illites (Tables 5 and 6) that formed were thus, high octahedral aluminum, low octahedral magnesium illites with limited iron.

The bulk chemistry of the limestones and dolomites gives an important clue to the differences between them. Fe^{+3} occupies the octahedral illite layer and, given the mineralogy, nowhere else. Analysis of Table 4 shows that all dolomites have higher Fe^{+3} than their corresponding limestone, indicating higher illite content in the dolomite. The inference is that dolomite pods had higher illite content, lower permeability and, more intense reducing conditions.

Significant amounts of NH_4^+ in the illites of associated limestones was not expected, but is reasonable. Limestone and dolomite samples were juxtaposed spatially (the dolomite occurring as pods) in field exposure and taken very near the sharp limestone/dolomite contact of the dolomite pods. Thus, NH_4^+ diffusing away from the zone of dolomitization into the bounding limestone would be incorporated into the illites of the limestone during

diagenesis. Sulfate reduction probably also occurred in the limestones around the dolomite. Small amounts of NH_3 produced by bacterial protein degradation associated with the limestone would be incorporated as NH_4^+ into associated illites. The NH_4 -illite present in the limestone of the Madison Formation probably resulted from the combined effect of diffusion of NH_4^+ away from the zone of sulfate reduction, where dolomitization was occurring and from sulfate reduction occurring in the limestones around the dolomites.

The mineralogy of the accessory minerals mirrors, in a scaled down way, the mineralogy of the Green River Formation (Slaughter and Mathews, 1984), where the intense, organically induced diagenesis produced pure diagenetic albite and microcline at the expense of three layer clay minerals. In zones of most intense bacterial sulfate reduction, CO_3^{-2} , H_2S and NH_3 concentrations were high enough to make it thermodynamically favorable for more magnesium to be incorporated in carbonates leaving less magnesium available for illite formation and more K^+ , NH_4^+ , Al and Si for microcline formation. The bacterial activity resulted in NH_4^+ -bearing microcline instead of NH_4^+ -illite, producing 7 times more microcline observed in the bulk mineralogy of the dolomites (ave. = 0.7 wt. %) than the limestones (ave. = 0.1 wt. %). Albite is observed in all dolomite (ave. = 2.1 wt. %) samples and 54% of the limestone samples (ave. = 0.5 wt. %). Diagenetic albite, like diagenetic microcline in the Madison Formation, is a result of the depletion of iron and magnesium due to incorporation into carbonates and illite and relatively high NH_4^+ and sodium concentrations in the pore waters. Magnesium is a necessary octahedral cation in montmorillonite clays. The formation of dolomite and illite precluded the formation of montmorillonite or mixed layer illite-montmorillonite, because there was no magnesium available to make these clays stable. Thus, albite became the stable sodium phase and forms to accommodate sodium in the diagenetic system in the

presence of K^+ or NH_4^+ . The combination of sodium and ammonium in the pore waters is important because ammonium has a low hydration energy and favors incorporation into a non-hydrated phase. A non-hydrated mineral, such as albite, can accommodate only very small amounts of ammonium with sodium in the albite crystal structure. The albite observed in the bulk mineralogy formed as a result of dolomite formation during sulfate reduction. This is why albite is 4 times as abundant in dolomite samples than limestone samples. Minor amounts of detrital albite probably acted as a nucleus for authigenic albite precipitation making the albite partially detrital and partially authigenic.

Dolomitization

The dolomite pods observed in the Madison Formation, like the dolomite in the Green River Formation, are interpreted to be a direct result of bacterial sulfate reduction or methanogenesis and bacterial protein hydrolysis and deamination of organic matter, initially preserved in the sediment. Dolomite, the thermodynamically stable carbonate in seawater, formed as a result of increased pH conditions in the sediments that were created by NH_3 , a natural base produced by protein hydrolysis and deamination during bacterial sulfate reduction or methanogenesis where CO_2 reduction is also occurring. The presence of authigenic NH_4^+ -illites and associated microcline and albite in the dolomites of the Madison Formation support the hypothesis that NH_3 produced in the zone of bacterial sulfate reduction or methanogenesis is vital to dolomitization. These authigenic phases confirm that organic matter was initially present in the Madison Formation and that diagenetic reactions occurred as a result of CO_2 , H_2S and NH_3 produced during diagenesis. The role of NH_3 is to increase pH of the pore fluids and subsequently increase the CO_3^{2-}/HCO_3^- ratio of the pore fluids, favoring carbonate precipitation. Dolomitization

had to occur while NH_3 was produced during bacterial sulfate reduction or methanogenesis because magnesium supply becomes a problem at depths where thermocatalytic (50°C or approximately 500-1000 meters) NH_3 begins evolution. An internal source of magnesium is required for dolomitization at these depths, which limits the amount of dolomite that can form. That dolomite forms in the zone of bacterial sulfate reduction or methanogenesis is further supported by the composition of the illite. The low octahedral magnesium, high octahedral aluminum observed in the illites is a result of magnesium incorporated into dolomite during sulfate reduction.

The lack of significant amounts of pyrite supports most iron being present in the illite of the limestones and dolomites. According to the hypothesis stated earlier, dolomitization occurring in the sulfate reducing zone means pyrite will be a significant mineral constituent if iron is present. Pyrite is barely detected in the Madison Formation dolomites except for one sample (9) which showed abundant iron oxide after pyrite in field exposure. The lack of pyrite is explained by the low iron content of Madison Formation sediments. The limited amount of iron in the system, due to almost no detrital mineral input into the Madison, prevented abundant pyrite formation and formation of more illite or illite with more octahedral iron. Consequently, most H_2S would have escaped the system as a slightly soluble gas with some remaining in solution as HS^- . The dolomite pods of the Madison Formation thus, represent zones where organic matter derived from marine plankton was preserved during sedimentation and where the production of NH_3 by protein hydrolysis and deamination in the zone of bacterial sulfate reduction produced the dolomite locally.

Carbon Isotopes

According to current theory, carbon isotope values for the Madison Formation dolomite show no indication of dolomitization in the zone of sulfate reduction or methanogenesis, even though mineralogic evidence supports a bacterial sulfate reduction origin. Based on previous work on organogenic dolomites (see section on previous work), one would expect dolomite formed in the sulfate reducing zone to show carbon isotope values around -15 ‰ PDB. Dolomites forming in the methanogenic zone would be expected to show values around +20 ‰.

The carbon isotope values, however, tell us that the dolomites formed by replacement of the pre-existing limestone deposited from a normal Mississippian marine environment. The carbonate ion incorporated in the replacement Madison dolomite is dominantly derived from the precursor calcite or aragonite and not carbonate ions in pore solutions produced during bacterial oxidation of organic matter. Carbon isotope values for carbonate shell material precipitated by organisms from sea water are near the value of seawater, which would give the replacement dolomite a similar value. The Madison Formation limestones have an average $\delta^{13}\text{C}$ of 0.9 ‰ PDB, the dolomites an average value of 1.3 ‰ PDB. Clearly, the carbon in the limestones will be conserved during dolomitization. The average value of 0.9 ‰ PDB, is typical of bulk marine sediment of biological origin (Land, 1989).

The dolomites that show carbon isotope values reflecting sulfate reduction or methanogenesis are dominantly dolomites that precipitate directly from solution (i.e. Deep Sea Drilling Project dolomites, supersaline parts of the Green River Formation dolomites and some Monterey Formation dolomites). Some dolomites of the Monterey Formation and those found in Deep Sea Drilling Project cores are "organogenic" dolomites that

precipitated from dolomite supersaturated diagenetic fluids below the depositional interface (various papers in Garrison, et al., 1984, and Kelts and McKenzie, 1982, respectively). The supersaturation of dolomite in these diagenetic fluids is a result of CO₂ produced by the bacterial oxidation of organic matter below the depositional interface, increasing the concentration of carbonate ions in solution. The dolomites show excessive positive and negative carbon isotope values reflecting incorporation of CO₂ derived from bacterial methanogenesis and sulfate reduction, respectively. The amount of replacement dolomite in these carbonate units are minor, since the sediments are dominantly detrital, but they also show carbon isotope values that support replacement in a sulfate reducing or methanogenic zone.

The minor amounts of replacement dolomite with anomalously high/low $\delta^{13}\text{C}$ in the dominantly detrital sediments of the Monterey Formation and Deep Sea Drilling Project cores suggests that solution chemistry will control carbon isotope values in replacement dolomites in rock systems that are dominated by detrital sediments. Conversely, $\delta^{13}\text{C}$ values of large amounts of replacement dolomite in dominantly carbonate sediment will be buffered by the precursor limestone, regardless of whether or not small amounts of directly precipitated, isotopically anomalous dolomite is present. This is supported by mass balance calculations (see Appendix C).

Clearly, many factors are important in determining the carbon isotope signature of dolomites. The sedimentary environment of dolomitization is an important factor influencing the carbon isotopic signature of the dolomite: for example, whether the dolomite formed in a carbonate platform environment or an environment dominated by detrital sedimentary input. In detritally dominated, organic-rich sediments, the dolomite carbon isotope values will reflect the pore solution values, whereas in carbonate platform

environments the carbon isotope values will reflect the precursor carbonate minerals. Although both environments can show evidence for organically induced dolomitization, only the organic-rich, detrital sediments will reflect this in carbon isotope values (Appendix C).

Thin Section Analysis

The planar-s texture of the dolomite in the Madison Formation suggests formation at temperature less than 50° C according to Sibley and Gregg (1987) and supports dolomitization during early diagenesis. The minor amounts of detrital minerals in the Madison Formation and presence of authigenic quartz in pore spaces further indicate that the accessory minerals present in the Madison Formation are dominantly authigenic with limited detrital character.

Cathodoluminescence

Cathodoluminescence of the Madison Formation dolomites show dull dolomite cores with some bright dolomite overgrowths lining dolomite crystals as rims in pore spaces or filled pores. The bright rims probably contain manganese, while the dull cores contain small amounts of iron. The dull cores are consistent with compositions determined for the dolomites. The bright dolomite does not occur within the dull dolomite crystal cores and suggests either manganese was incorporated into the dolomite toward the end of dolomitization or iron was no longer incorporated. Texturally, the bright dolomite appears to have precipitated from solution and used the replacement dolomite as a nuclei for growth. In the Madison Formation, the amount of dolomite precipitating from solution is

volumetrically small (<5%) and thus, should not produce large carbon isotope variations in bulk sample determinations.

Strontium Isotopes

$^{87}\text{Sr}/^{86}\text{Sr}$ ratio of sample 10 showed a value of .709165 +/- .00005 which corresponds with Cambro-Ordovician seawater and modern seawater (Burke, et al., 1982), and many types of groundwater. The value for Kinderhookian deposition is approximately .7079 (Popp, et al., 1986). Since there is no evidence of detrital carbonate input (rounded dolomite crystals or grains) that could have been derived from the underlying Cambrian Gallatin or Ordovician Bighorn Formations, the Sr ratio could reflect a flow of groundwater with this signature.

CONCLUSIONS

Dolomite pods and laterally extensive thin beds of the Mississippian Madison Formation formed during early diagenesis in the zone of bacterial sulfate reduction or methanogenesis and are the result of NH_3 liberated during enzymatic protein hydrolysis and deamination. The NH_3 was important in dolomitization because the NH_3 acted to locally raise pH which in turn increased the $\text{CO}_3^{2-}/\text{HCO}_3^-$ ratio of pore waters making replacement dolomitization of the sediments favorable. The dolomite pods and associated limestones of the Madison Formation thus, represent volumes where organic matter was preserved during deposition of the Madison Formation.

The role of NH_3 in dolomitization is supported by the presence of NH_4^+ -illites associated with the dolomite pods of the Madison Formation. The presence of NH_4^+ -illite confirms that organic matter was initially present during deposition of Madison sediments. The authigenic NH_4^+ -illites associated with the dolomite pods of the Madison Formation formed in the zone of bacterial sulfate reduction or methanogenesis, while NH_3 was being liberated and dolomitization occurred. Dolomitization must have occurred in the zone of bacterial action because deeper burial would have limited Mg^{+2} for dolomitization.

Associated mineral compositions also support dolomitization in the zone of bacterial sulfate reduction or methanogenesis. The illite octahedral layer is aluminum rich and magnesium poor which reflects formation in the shallow zone of bacterial sulfate reduction or methanogenesis during dolomitization. Illite is most stable with iron and magnesium in octahedral sites. During extreme sulfate reduction most iron reduces and incorporates into pyrite and carbonate minerals, leaving almost no iron for illite or illite/smectite formation. At the same time, magnesium that could be used for illite or smectite formation is used to

make dolomite. The result would be an iron and magnesium poor illite that must have formed in the zone of sulfate reduction prior to and while dolomitization was occurring. During less intense reduction, illite contemporaneous with dolomite would retain at least part of its Fe^{+3} but not magnesium. The Fe^{+3} of the illite indicates reduction, but not intense reduction as in the Green River Formation. The illite composition reflects the most stable illite that could form in the diagenetic conditions that prevailed in the Madison Formation, and is a product of the ammonium concentrations created by protein deamination in the zone of bacterial sulfate reduction. NH_4^+ is required for illite formation because of the low potassium content of the sediments.

The increase in microcline observed in the bulk mineralogy of the dolomites relative to the limestones can be the result of more intense bacterial sulfate reduction and bacterial protein hydrolysis and deamination, as in the Green River Formation, making microcline (NH_4^+ -microcline) stable over NH_4^+ -illite in the system. Where bacterial sulfate reduction was more intense, greater amounts of NH_3 , CO_2 and H_2S are produced during diagenesis resulting in more iron and magnesium, needed for illite stability, being incorporated into pyrite and carbonate minerals making microcline stable with respect to diagenetic illite. Similar mineralogies are expected in the methanogenic zone except sulfides will be limited. The diagenetic microcline precipitated on detrital microcline as a nucleus, making the microcline observed in the samples seem dominantly authigenic, and because of the low potassium content of the Madison Formation, ammonium-bearing. The microcline identified in the samples is actually a mixed microcline- NH_4^+ -microcline phase.

Carbon isotope values for limestones and dolomites of the Madison Formation suggest carbon isotope data cannot be used as strict indicators of organogenic carbonate precipitation in the zone of bacterial sulfate reduction or methanogenesis. Instead, the

carbon isotopes, determine whether the dolomite precipitated from solution, formed by replacement of a carbonate mineral precursor in a detrital dominated environment, or replaces limestone. In a detritally dominated system, the amount of limestone deposited is limited and dolomite precipitates from solution with only minor replacement dolomitization occurring. The dolomites in this setting will have carbon isotopes reflecting carbon values for sulfate reduction, methanogenesis, or thermocatalytic organic degradation, because the carbonate ion incorporated into the dolomite from pore solutions will have been derived from bacterial respiration or thermocatalytic degradation of organic matter. In platform carbonate environments, carbon isotope values will reflect the precursor limestone, because the dolomite in this environment forms by replacement and incorporates carbonate ions dominantly from the precursor mineral and seawater instead of from the pore waters. These conclusions are supported by mass balance calculations. Consideration of whether the environment of formation for dolomite is dominantly detrital or a carbonate platform, and whether the dolomite is precipitating from solution or by replacement, becomes the important controlling factors in determining dolomite carbon isotope values.

The presence of organogenic dolomites in a normal marine environment suggests many platform and shelf dolomites could have an organogenic origin. Where protein-rich organic matter is preserved and a Mg^{+2} source is available, dolomitization is possible. The laterally and vertically extensive platform dolomites that define the "dolomite problem" should be re-evaluated in light of these conclusions. Because bacterial sulfate reduction occurs during early diagenesis at shallow depths, favorable chemical conditions (pH) can be established for dolomitization in the presence of a substantial Mg^{+2} source (seawater).

The results of this study also show mineral indicators are more reliable in determining the influence of organic matter in dolomitization than interpretations based strictly on

carbon isotope values. The accessory minerals present and their compositions should be carefully evaluated when analysis of chemical conditions for dolomitization are studied, because these minerals give insight into diagenetic conditions that carbon isotopes cannot provide.

REFERENCES CITED

- Adams, J.E. and M.L. Rhodes, 1960. Dolomitization by seepage refluxation. American Association of Petroleum Geologists Bulletin, **44**, 1912-1920.
- Alderman, A.R. and H.C.W. Skinner, 1957. Dolomite sedimentation in the southeast of South Australia. American Journal of Science, **255**, 561-567.
- Aharon, Paul, Yehoshua Kolodny and Eytan Sass, 1977. Recent hot brine dolomitization in the "Solar Lake", Gulf of Elat, isotopic, chemical and mineralogical study. Journal of Geology, **85**, 27-48.
- Badiozamani, K., 1973. The Dorag dolomitization model-application to the Middle Ordovician of Wisconsin. Journal of Sedimentary Petrology, **43**, 965-984.
- Baker, Paul A. and Stephen J. Burns, 1985. Occurrence and formation of dolomite in organic-rich continental margin sediments. American Association of Petroleum Geologists Bulletin, **69** (11), 1917-1930.
- Baker, Paul A. and M. Kastner, 1981. Constraints on the formation of sedimentary dolomite. Science, **213**, 214-216.
- Beales, F.W. and J.W. Hardy, 1980. Criteria for the recognition of diverse dolomite types with an emphasis on studies of host rocks for Mississippi Valley Type ore deposits. In Zenger, D.H., Dunham, J.B. and Ethington, R.L. (eds.), Concepts and Models of Dolomitization. Society of Economic Paleontologists and Mineralogists Special Publication Number 28, 197-214.
- Bramlette, M.N., 1946. The Monterey Formation of California and the origin of its siliceous rocks. United States Geologic Survey Professional Paper 212, 57 p.
- Budai, Joyce M., Kyger C. Lohmann and James Lee Wilson, 1987. Dolomitization of the Madison Group, Wyoming and Utah Overthrust Belt. American Association of Petroleum Geologists Bulletin, **71** (8), 909-924.
- Burke, W.H., R. E. Denison, E. A. Heatherington, R. B. Koepnick, N. F. Nelson and J. B. Otto, 1982. Variation of seawater $^{87}\text{Sr}/^{86}\text{Sr}$ throughout Phanerozoic time. Geology **10**, 515-519.
- Burns, Stephen J. and Paul A. Baker, 1987. A geochemical study of dolomite in the Monterey Formation, California. Journal of Sedimentary Petrology, **57** (1), 128-139.
- Bush, P., 1973. Some aspects of the diagenetic history of the sabkha in Abu Dahbi, Persian Gulf. In B.H. Purser, (ed.), The Persian Gulf-Holocene carbonate sedimentation and diagenesis in a shallow epicontinental sea. Springer-Verlag, New York, 471p.

- Butler, G.P., 1969. Modern evaporite deposition and geochemistry of co-existing brines, the sabkha, Trucial Coast, Arabian Gulf. *Journal of Sedimentary Petrology*, **39**, 70-89.
- Choquette, P.W. and R.P. Steinen, 1980. Mississippian non-supratidal dolomite, Ste. Genevieve Limestone, Illinois Basin: Evidence for mixed water dolomitization. *In* Zenger, D.H., J.B. Dunham and R.L. Ethington (eds.), *Concepts and Models of Dolomitization*. Society of Economic Paleontologists and Mineralogists Special Publication Number 28, 215-236.
- Claypool, G.E., and I.R. Kaplan, 1974. The origin and distribution of methane in sediments. *In* I.R. Kaplan (ed.), *Natural Gases in Marine Sediments*. Plenum, New York, 99-139.
- Compton, John S., 1988. Degree of supersaturation and precipitation of organogenic dolomite. *Geology*, **16**, 318-321.
- Cooper, James E., 1986. Determination of total nitrogen in oil shale. *Analytical Chemistry*, **58**, 1571-1572.
- Cooper, James E. and W.S. Evans, 1983. Ammonium nitrogen in Green River Formation oil shale. *Science*, **219**, 492-493.
- Davies, G.R., 1979. Dolomite reservoir rocks: processes, controls, porosity development. *In* *Geology of Carbonate Porosity*. American Association of Petroleum Geologists Short Course, note series no.11, Houston, C1-C17.
- Deffeyes, K.S., F. A. Lucia and P. K. Weyl, 1965. Dolomitization of Recent and Plio-Pleistocene sediments by marine evaporite waters on Bonaire, Netherlands Antilles. *In* Pray, C.C. and R.C. Murray (eds.), *Dolomitization and Limestone Diagenesis*. Society of Economic Paleontologists and Mineralogists Special Publication Number 13, 71-89.
- de Groot, K., 1973. Geochemistry of tidal flat brines at Umm Said, S.E. Qatar, Persian Gulf. *In* Purser, B.H. (ed.), *The Persian Gulf-Holocene Carbonate Sedimentation in a Shallow Epicontinental Sea*. Springer-Verlag, New York, 337-394.
- Dunham, R. J., 1962. Classification of carbonate rocks according to depositional texture. *In* Haun, W. E. (ed), *Classification of carbonate rocks*. *Memoirs of the American Association of Petroleum Geologists* **1**, 108-121.
- Dunham, J.B. and E.R. Olsen, 1978. Diagenetic dolomite formation related to Paleozoic paleogeography of the Cordilleran miogeosyncline in Nevada. *Geology*, **6**, 556-559.
- Durand, B. (ed.), 1980. *Kerogen*. Editions Technip, Paris, 519p.
- Folk, R. L., 1959. Practical petrographic classification of limestones. *American Association of Petroleum Geologists Bulletin* **43**, 1-38.

- Folk, R.L. and L.S. Land, 1975. Mg/Ca ratio and salinity: two controls over crystallization of dolomite. *American Association of Petroleum Geologists Bulletin*, **59**, 60-68.
- Friedman, Irving and K.J. Murata, 1979. Origin of dolomite in Miocene Monterey Shale and related formations in the Temblor Range, California. *Geochimica et Cosmochimica Acta*, **43**, 1357-1365.
- Garrison, R.E., Miriam Kastner and Donald Zenger (eds.), 1984. Dolomites of the Monterey Formation and other Organic-Rich Units. Pacific Section, Society of Economic Paleontologists and Mineralogists Special Publication, 215p.
- Gebelein, Conrad D. and Paul Hoffman, 1973. Algal origin of dolomite laminations in stromatolitic limestone. *Journal of Sedimentary Petrology*, **43** (3), 603-613.
- Gieskes, Joris M., 1973. Interstitial Water Studies, Leg 15 - alkalinity, pH, Mg, Ca, Si, PO₄⁻ and NH₄⁺. *In* B.C. Heezen, I.D. McGregor, et al., Initial Reports on the Deep Sea Drilling Project, **20**, 813-829.
- Geiskes, Joris M., B. Nevsky and A. Chain, 1981. Interstitial Water Studies, Leg 63. *In* R. Yeats, B. Haq, et al., Initial Reports of the Deep Sea Drilling Project, **63**, 623-629.
- Geiskes, Joris M., Henry Elderfield, James R. Lawrence, Jeff Johnson, Barbara Myers and Andrew Campbell, 1982. Geochemistry of Interstitial Waters and Sediments, Leg 64, Gulf of California. *In* J.R. Curry, and D.G. Moore, et al., Initial Reports on the Deep Sea Drilling Project, **64**, 675-694.
- Geiskes, Joris M., K. Johnston, M. Boehm and M. Nohara, 1984. Interstitial Water studies, Deep Sea Drilling Project, Leg 75. *In* W. Hay, J.C. Sibnet, et al., Initial Reports on the Deep Sea Drilling Project, **75**, 659-663.
- Given, R. K. and B. H. Wilkinson, 1987. Dolomite abundance and stratigraphic age: constraint on rates and mechanisms of Phanerozoic dolostone formation. *Journal of Sedimentary Petrology*, **57**, 1068-1078.
- Goodell, H.G. and R.K. Garman, 1969. Carbonate geochemistry of Superior deep test well, Andros Island, Bahamas. *American Association Petroleum Geologists Bulletin*, **53**, 513-536.
- Gregg, J.M., 1985. Regional epigenetic dolomitization in the Bonneterre dolomite (Cambrian), northeast Missouri. *Geology*, **13**, 503-506.
- Gregg, J.M. and R.D. Hagni, 1987. Irregular cathodoluminescent banding in late dolomite cements: evidence from complex faceting and metalliferous brines. *Geologic Society of America Bulletin*, **98**, 86-91.

- Griffin, D.G., 1965. The Devonian Slave Point, Beaver Hill Lake, and Muskwa Formations of northeastern British Columbia and adjacent areas. *British Columbia Dept. Mines and Petroleum Resources Bulletin*, **50**, 90p.
- Guanatilaka, A., A. Saleh, A. Al-Teneemi and N. Nassar, 1984. *Nature*, **311**, 450.
- Gutschick, R.C., C. A. Sandberg and M. J. Sando, 1980. Mississippian shelf margin and carbonate platform from Montana to Nevada. *In* T.D. Fouch and E.D. Magathan (eds.), *Paleozoic paleogeography of the west-central United States, Rocky Mountain paleogeography symposium 1*. Rocky Mountain Section Society of Economic Paleontologists and Mineralogists, 111-128.
- Hallum, M. and H.P. Eugster, 1976. Ammonium silicate stability relations. *Contributions to Mineralogy and Petrology*, **57**, 227.
- Hansaw, B.B., W. Back and R. G. Dieke, 1971. A geochemical hypothesis for dolomitization by groundwater. *Economic Geology*, **66**, 710-724.
- Hardy, Laurence A., 1987. Perspectives Dolomitization: a critical review of some current views. *Journal of Sedimentary Petrology*, **57** (1), 166-183.
- Hein, James R., James R. O'Neil and Marjorie G. Jones, 1979. Origin of authigenic carbonates in sediments from the deep Bering Sea. *Sedimentology*, **26**, 681-705.
- Hower, J., Eric V. Eslinger, Mark E. Hower and Edward E. Perry, 1976. Mechanism of burial metamorphism of argillaceous sediments: 1. Mineralogical and chemical evidence. *Geologic Society of America Bulletin*, **87**, 725-737.
- Hsu, K.J., 1966. Origin of dolomite in sedimentary sequences: a critical analysis. *Mineralium Deposita*, **2**, 133-138.
- Hsu, K. J. and J. Schneider, 1969. Progress report on dolomitization hydrology of Abu Dahbi sabkhas, Arabian Gulf. *In* Purser, B.H. (ed.), *The Persian Gulf-Holocene Carbonate Sedimentation in a Shallow Epicontinental Sea*. Springer-Verlag, New York, 409-422.
- Hsu, K. J. and C. Siegenthaler, 1969. Preliminary experiments on hydrodynamic movement induced by evaporation and their bearing on the dolomite problem. *Sedimentology*, **12**, 11-25.
- Huc, A. Y., B. Durand, and J. C. Monin, 1978. Humic compounds and kerogen in cores from Black Sea sediments. Leg42B-Holes 379A, B and 380A. *In* Initial Reports of the Deep Sea Drilling Project, XL11, part 2, 737-748.
- Illing, L.V., 1959. Deposition and diagenesis of some upper Paleozoic carbonate sediments in western Canada. 5th World Petroleum Congress, New York, proceedings, section 1, 23-52.

- Illing, G.U., A. J. Wells and J. C. M. Taylor, 1965. Penecontemporary dolomite in the Persian Gulf. *In* Pray, L.C. and R.C. Murray (eds.), *Dolomitization and Limestone Diagenesis*. Society of Economic Paleontologists and Mineralogists Special Publication Number 13, 89-111.
- Irwin, Hillary, 1980. Early diagenetic carbonate precipitation and pore fluid migration in the Kimmeridge Clay of Dorset, England. *Sedimentology*, **27**, 577-591.
- Jodry, R.L., 1969. Growth and dolomitization of Silurian reefs, St. Clair County, Michigan. *American Association of Petroleum Geologists Bulletin*, **53**, 957-981.
- Kastner, M., 1984. Control of dolomite formation. *Nature*, **311**, 410-411.
- Kelts, Kerry and Judith A. McKenzie, 1982. Diagenetic dolomite formation in Quaternary anoxic diatomaceous muds of Deep Sea Drilling Project Leg 64, Gulf of California. *In* J.R. Curry, D.G. Moore, et al., *Initial Reports on the Deep Sea Drilling Project*, **64**, 553-569.
- Kendall, A.C., 1977. Origin of dolomite mottling in Ordovician limestones from Saskatchewan and Manitoba. *Canadian Society of Petroleum Geology Bulletin*, **25**, 480-504.
- King, R.H., 1947. Sedimentation in the Permian Castile Sea. *American Association Petroleum Geologists Bulletin*, **31**, 470-477.
- Kinsman, D.J.J., 1966. Gypsum and anhydrite of Recent age, Trucial Coast, Persian Gulf. *In* Raw, J.L. (ed.), *Second Symposium on Salt, Volume 1*. Northern Ohio Geologic Society, 302-326.
- Kocurko, J.M., 1979. Dolomitization by spray zone brine seepage San Andres, Columbia. *Journal of Sedimentary Petrology*, **49**, 209-214.
- Land, L.S., 1973. Contemporaneous dolomitization of Middle Pleistocene reefs by meteoric water, North Jamaica. *Marine Science*, **23**, 84-92.
- Land, Lynton S., 1985. The origin of massive dolomite. *Journal of Geologic Education*, **33**, 112-125.
- Land, Lynton S., 1989. *Handbook of Environmental Geochemistry*, v. 3.
- Land, L.S., M. R. I. Salem and D. W. Morrow, 1975. Paleohydrology of ancient dolomites - geochemical evidence. *American Association of Petroleum Geologists Bulletin*, **59**, 1602-1625.
- Lippman, F., 1973. *Sedimentary Carbonate Minerals*. Springer Verlag, New York, 228p.

- Machemer, Steven D., and Ian Hutcheon, 1988. Geochemistry of early carbonates cements in the Cardium Formation, Central Alberta. *Journal of Sedimentary Petrology*, **58** (1), 136-147.
- MacKenzie, J.A., et al., 1980. Movement of subsurface waters under the sabkha, Abu Dhabi, UAE, and its relation to evaporite dolomite genesis. *In* Zenger, D.H., J.B. Dunham and R.L. Ethington (eds.), *Concepts and Models of Dolomitization*. Society of Economic Paleontologists and Mineralogists Special Publication Number 28, 11-30.
- Mattes, B.W. and E.W. Mountjoy, 1980. Burial dolomitization of the upper Devonian Miette Buildup, Jasper National Park, Alberta. *In* Zenger, D.H., J.B. Dunham and R.L. Ethington (eds.), *Concepts and Models of Dolomitization*. Society of Economic Paleontologists and Mineralogists Special Publication Number 28, 259-297.
- Meyers, W.J. and K.C. Lohman, 1983. Carbon isotope data for Mississippian, previously unpublished. *In* James, N.P. and P.W. Choquette, 1984. *Diagenesis 6. Limestones-The Seafloor diagenetic environment*. Geoscience Canada, **10** (4), 162-179.
- Moore, G.W. and J.M. Gieske, 1980. Interaction between sediment and interstitial water near the Japan Trench, Leg 57, Deep Sea Drilling Project. *In* M. Lee, L.N. Stout, et al., *Initial Reports on the Deep Sea Drilling Project*, **56-57**, 1268-1276.
- Morrow, D.W., 1982a. Diagenesis 1. Dolomite-Part 1: The chemistry of dolomitization and dolomite precipitation. *Geoscience of Canada*, **9** (1), 5-13.
- Morrow, D.W., 1982b. Diagenesis 2. Dolomite Part 2: Dolomitization models and ancient dolostones. *Geoscience of Canada*, **9** (2), 95-107.
- Muller, S. and G. Teitz, 1971. Dolomite relacing "cement A" in biocalcarenites from Fuerteventura, Canary Islands, Spain. *In* Bricker, D.P. (ed.), *Carbonate Cements*. Baltimore, Johns Hopkins Press, 376p.
- Muir, M., D. Lock and C. Von der Brock, 1980. The Coorong Model for penecontemporaneous dolomite formation in the Middle Proterozoic McArthur Group, Northern Territory, Australia. *In* Zenger, D.H., J.B. Dunham and R.L. Ethington (eds.), *Concepts and Models of Dolomitization*. Society of Economic Paleontologists and Mineralogists Special Publication Number 28, 51-68.
- Murray, R.C., 1969. Hydrology of south Bonaire, Netherlands Antilles-a rock selective dolomitization model. *Journal of Sedimentary Petrology*, **39**, 987-1035.
- McHargue, Timothy R. and Rex C. Price, 1982. Dolomite from clay in argillaceous or shale-associated marine carbonates. *Journal of Sedimentary Petrology*, **52** (3), 873-886.

- Nissenbaum, A. B., B. J. Presley, and I. R. Kaplan, 1972. Early Diagenesis in a reducing Fjord, Saanich Inlet, British Columbia - I. Chemical and isotopic changes in major components of interstitial water. *Geochemica et Cosmochemica Acta*, 1007.
- Patterson, R.J., 1972. Hydrology and carbonate diagenesis of a coastal sabkha in the Persian Gulf, Ph.D. Thesis, Princeton Univ., Princeton, N.J., 498p.
- Patterson, R.J. and D.J.J. Kinsman, 1981. Hydrologic framework of a sabkha along the Arabian Gulf. *American Association of Petroleum Geologists Bulletin*, 65, 1457-1475.
- Patterson, R.J., and D.J.J. Kinsman, 1982. Formation of diagenetic dolomite in coastal sabkha along Arabian (Persian) Gulf. *American Association of Petroleum Geologists Bulletin*, 66 (1), 28-43.
- Perry, E.A., Jr., and J. Hower, 1970. Burial diagenesis of Gulf Coast pelitic sediments. *American Association of Petroleum Geologists Bulletin*, 56, 2013-2021.
- Pierre, Catherine, Luc Ortlieb and Alain Person, 1984. Supratidal evaporitic dolomite at Ojo De Liebre Lagoon: Mineralogical and isotopic arguments for primary crystallization. *Journal of Sedimentary Petrology*, 54 (4), 1049-1061.
- Pisciotta, K.A., and J.J. Mahoney, 1981. Isotopic survey of diagenetic carbonates, Deep Sea Drilling Project Leg 63. In Yeats, R., B. Haq, et al., Initial Reports on the Deep Sea Drilling Project, 63, 595-609.
- Popp, Brian N., Frank A. Podosek, Joyce C. Brannon, Thomas F. Anderson and Jean Pier, 1986. $^{87}\text{Sr}/^{86}\text{Sr}$ ratios in Permo-Carboniferous sea water from the analyses of well-preserved brachiopod shells. *Geochimica et Cosmochimica Acta*, 50, 1321-1328.
- Presley, B. J., and I. R. Kaplan, 1968. Changes in Dissolved Sulfate, calcium and carbonate from interstitial water near shore sediments. *Geochimica et Cosmochimica Acta*, 32, 1037-1048.
- Presley, Bob J., James Culp, Chari Petrowski and I. R. Kaplan, 1973. Interstitial Water Studies, Leg 15 - Major ions Br, Mn, NH_3 , Li, B, Si and ^{13}C . In B.C. Heezen, I.D. McGregor, et al., Initial Reports on the Deep Sea Drilling Project, 20, 805-809.
- Radslovich, E.W., 1962. The cell dimensions and symmetry of layer lattice silicates, regression relations. *American Mineralogist*, 47, 617-636.
- Randazzo, A.F. and E.W. Hickey, 1978. Dolomitization in the Floridan Aquifer. *American Journal of Science*, 278, 1177-1184.
- Rashid, M. A., 1985. *The Geochemistry of Marine Humic Compounds*. Springer-Verlag, New York, 300p.

- Rosen, Micheal R., et al., 1988. Sedimentology, mineralogy and isotopic analysis of Pellet Lake, Coorong Region, South Australia. *Sedimentology*, **35**, 105-122.
- Sando, W.J., 1976. Mississippian history of the Rocky Mountain Region, United States Geologic Survey Journal of Research, **4**, 317-338.
- Shimmield, G.B. and N.B. Price, 1984. Recent dolomite formation in hemipelagic sediments off Baja California, Mexico. In Garrison, Robert E., Miriam Kastner and Donald H. Zenger (eds.), *Dolomites of the Monterey Formation and other Organic-Rich Units*. Pacific Section Society of Economic Paleontologists and Mineralogists, **41**, 5-18.
- Sibley, Duncan F. and Jay M. Gregg, 1987. Classification of dolomite rock textures. *Journal of Sedimentary Petrology*, **57**, 967-975.
- Simoneit, Bernd R.T. and G.W. Bode, 1982. Appendix II; carbon/carbonate and nitrogen analysis, Leg 64, Gulf of California. In J.R. Curry, D.G. Moore, et al., **64**, 1303-1305.
- Slaughter, M., 1985. Quantitative mineral analysis of clays and other minerals. In press, Twenty Second Annual Clay Minerals Conference, Denver, Colorado, 44p.
- Slaughter, M. and A. Mathews, 1984. Mineralogy and Geochemistry of the Green River Formation, Colorado Core Hole No. 1, Piceance Creek Basin, Colorado. Department of Energy Report of Investigation, Volumes I and II, U. S. Department of Energy, office of Fossil Energy, Morgantown Energy Technology Center, Laramie Project Office, Laramie, Wyoming, 894 p.
- Spotts, J.H. and S.R. Silverman, 1966. Organic dolomite from Point Fermin, California. *American Mineralogist*, **51**, 1144-1155.
- Stevenson, F.J., 1962. *Geochimica et Cosmochimica Acta*, **26**, 797.
- Stevenson, F.J. and A.S.P. Dahriwal, 1959. *Soil Sci. Society Proceedings*, **23**, 121.
- Strickland, John W., 1957. Summary of Mississippian and Devonian Stratigraphy, Wind River Basin, Wyoming. Twelfth Annual Field Conference-1957, 20-29.
- Sweeney, M., P. Turner and D. J. Vaughan, 1987. The Marl Slate: a model for the precipitation of calcite, dolomite and sulfides in a newly formed anoxic sea. *Sedimentology*, **34**, 31-48.
- Tissot, B.P. and D.H. Welte, 1984. *Petroleum Formation and Occurrence*: Springer-Verlag, New York, 609p.
- Von der Broch, C.C., 1976. Stratigraphy and formation of Holocene dolomite carbonate deposits on the Coorong area, South Australia. *Journal of Sedimentary Petrology*, **46**, 952-966.

- Von der Broch and D.E. Lock, 1979. Geologic significance of Coorong dolomites. *Sedimentology*, **26**, 813-824.
- Von der Broch, D. E. Lock, 1975. Groundwater formation of dolomite in Coorong region of South Australia. *Geology*, **3**, 283-285.
- Wanless, H.R., 1979. Limestone response to stress: Pressure solution and dolomitization. *Journal of Sedimentary Petrology*, **49**, 437-462.
- Waples, D.W., 1985. *Geochemistry in Petroleum Exploration*. IHRDC, Boston, 33-38.
- Zenger, Donald H., 1976. Dolomitization and dolomite "dikes" in the Wyman Formation (Precambrian), Northeastern Inyo Mountains, California. *Journal Sedimentary Petrology*, **46** (3), 457-462.
- Zenger, Donald H., 1983. Burial dolomitization in the Lost Burro Formation (Devonian), east-central California, and the significance of late diagenetic dolomitization. *Geology*, **11**, 519-522.

APPENDIX A Thin Section Descriptions

Sample numbers are displayed with location first and limestone (L) or dolomite (D) following at the beginning of each thin section description. Classification of each thin section according to Dunham, Folk and Sibley (for dolomites), with descriptions and interpretations, follow the sample number.

1 L

Classification:

Dunham - crinoidal biopackstone
Folk - crinoidal biomicrite

Description:

Crinoid spines, plates, arthropod fragments, brachiopod fragments, cement filled mollusc molds, coral fragments (?), foraminifera fragments (?), sponge spicules (?), micritized ooides and unidentifiable skeletal fragments set in a mud matrix. Many grains are partially to completely micritized. The fragments appear randomly oriented with no apparent preferred orientation or bedding. Silicification has occurred in some echinoderm fragments. There is some opaque material and quartz and/or feldspar grains present, also.

Interpretation:

The diverse fauna suggests deposition in a normal marine environment. Silicification occurred after deposition. The well rounded quartz/feldspar grains are detrital.

1 D

Classification:

Dunham - mostly dolomitized crinoidal biopackstone
Folk - mostly dolomitized crinoidal biomicrite
Sibley and Gregg - moldic unimodal planar-s dolomite

Description:

Dominantly dolomite, containing some non-dolomitized echinoderm fragments and mollusc, echinoderm and brachiopod molds. There is a coral present that contains some micritic dolomite and iron stained calcite around the edges. The dolomite is mostly subhedral and appears dirty throughout, although some rhombs have only dirty cores. There are some fine sulfides present. Very minor amounts of quartz filling intercrystalline pores and some quartz and/or feldspar grains are present. The calcite occurs intercrystalline to the dolomite rhombs. It appears as if the dolomite is "biting" into the calcite. The edges of some dolomite rhombs are also calcitic.

Interpretation:

Dolomitization occurred in a reducing environment as is indicated by the presence of sulfides. The cloudiness of the dolomite is the result of calcite inclusions in the dolomite. The subhedral texture of the dolomite suggests formation from solutions supersaturated with respect to dolomite but, below critical supersaturation and below the critical roughening temperature of approximately 50° C. Above these critical parameters, species are randomly added to the surface of the growing crystal, producing nonplanar crystal interfaces. The well rounded quartz and/or feldspar grains are detrital, whereas the intercrystalline quartz is authigenic.

2 L**Classification:**

Dunham - micritized crinoidal biopackstone
Folk - micritized crinoidal biomicrite

Description:

Contains echinoderm, brachiopod and arthropod fragments, along with micritized ooids and foraminifera set in a mud matrix. The sample is highly micritized, making grains hard to distinguish. Silica replaces some crinoids. Some interparticle space appears to be filled with sparry calcite that has been partially micritized. The rest of the pores are filled with micrite that has been partially dolomitized. Some organic staining with some sulfides is present.

Along the limestone/dolomite boundary, the occurrence of dolomite is sharp although significant amounts of calcite occur in the first centimeter of dolomite. At the boundary, calcite occurs as partially dolomitized grains and cement.

Interpretation:

Deposition occurred in a normal marine environment as suggested by the diverse fauna. Silicification occurred after deposition.

2 D**Classification:**

Dunham - bio dolostone
Folk - bio dolomite
Sibley and Gregg - unimodal planar-s dolomite

Description:

The dolomite is unimodal and subhedral. Inclusions of calcite give the dolomite a dirty appearance. The more inclusions, the dirtier the appearance. Dolomite appears to bite into the intercrystalline calcite. Some echinoderms are preserved nonmimically. There is also some opaque matter present consisting of organic matter and sulfides. There are minor amounts of quartz filling intercrystalline pore space.

Interpretation:

The presence of sulfides suggest dolomite formed in a reducing environment. The subhedral texture suggests dolomite precipitated from a supersaturated solution but, below critical supersaturation and below the critical roughening temperature of approximately 50° C. Quartz is authigenic, precipitating after dolomitization.

3 L**Classification:**

Dunham - partially dolomitized crinoidal biopackstone
Folk - partially dolomitized crinoidal biomicrite

Description:

Contains echinoderms, brachiopods, arthropods, mollusc molds, algae (?), foraminifera (?) set in a mud matrix. The sample is highly micritized and partially dolomitized making some grains hard to identify and giving the slide a dirty appearance. Some dolomite forms within echinoderm fragments and bites into other grains. A small amount of opaque material is present. Some silicification of skeletal grains has occurred.

Interpretation:

Deposition occurred in a normal marine environment as is suggested by the diverse fauna present. Silicification occurred after deposition.

3 D**Classification:**

Dunham - dolomitized biopackstone
Folk - dolomitized biomicrite
Sibley and Gregg - unimodal nonplanar dolomite

Description:

Unimodal and dominantly nonplanar with some planar-s crystal boundaries. The porosity is dominantly moldic with mollusc and echinoderm molds present. The dolomite is dirty, reflecting the presence of calcite inclusions within the dolomite. There is a small amount of organic matter present and very few sulfides. Minor amounts of intercrystalline quartz is present.

Interpretation:

The dolomite precipitated in a reducing environment, as is suggested by the the presence of very minor sulfides. The subhedral texture suggests precipitation occurred from a solution supersaturated with respect to dolomite but, below critical supersaturation and the critical roughening temperature of approximately 50° C (the temperature above which crystal growth occurs randomly on the surface). The quartz is authigenic, precipitating after dolomitization.

4 L

Classification:

Dunham - pelloidal biopackstone
Folk - pelloidal biosparite

Description:

Contains dominantly micritized grains which appear to comprise echinoderms, brachiopods, molluscs, arthropods, foraminifera, intraclasts, ooids and pelloids. The pelloids are not uniform in size or shape. Some echinoderms and brachiopods are partially silicified. There are some organic matter and well rounded quartz and/or feldspar grains present.

Interpretation:

The diverse fauna suggests deposition in a normal marine environment. The nonuniform size and shape of the pelloids suggests they are micritized grains. Partial silicification of echinoderms and brachiopods occurred after deposition. The quartz and/or feldspar grains are detrital.

4 D

Classification:

Sibley and Gregg - unimodal planar-s

Description:

The dolomite is unimodal and subhedral. There are no obvious grain relicts present. Calcite inclusions make the dolomite appear dirty. Dolomite appears to bite into intercrystalline calcite. There are very minor amounts of sulfides present and some organic matter. Quartz is present in intercrystalline pore space.

Interpretation:

The presence of sulfides suggests the dolomite precipitated in a reducing environment. The subhedral texture suggests the dolomite precipitated from dolomite supersaturated solutions, but below critical supersaturation and the critical roughening temperature which is approximately 50° C. The intercrystalline quartz is authigenic.

5 L

Classification:

Dunham - pelloidal biopackstone
Folk - pelloidal biomicrite

Description:

Sample contains highly micritized grains including echinoderms, brachiopods, foraminifera, arthropods (?) and some indistinguishable micritized debris. The

indistinguishable micritized debris varies in size and shape. The micritized grains are rimmed by spar cement. Overall grain size is constant with a few of the larger grains appearing to be intraclasts. Laminations are present near where dolomite begins to appear. There is some sulfides associated with the dolomite. There is some organic matter present in both the limestone and dolomite. Partial silicification of skeletal grains has occurred. Some well rounded quartz\feldspar grains are present.

Interpretation:

The diverse fauna suggests deposition in a normal marine environment. The various sizes and shapes of the pelloids suggests they are not fecal in origin but, micritized grains. The laminations may be algal in origin. Silicification occurred after deposition. The quartz and/or feldspar grains are detrital.

5 D

Classification:

- Dunham - dolomitized biopackstone
- Folk - dolomitized biomicrite
- Sibley and Gregg - unimodal planar-s

Description:

Unimodal, subhedral and shows nonmimic replacement of crinoid and mollusc fragments. Dolomite that fills some molds is clear, slightly coarser and shows some iron staining compared to the iron free, dirty, calcite inclusion-filled dolomite that makes up the bulk of the slide. The crystal boundaries of the dolomite are diffuse, because of the large number of calcite inclusions concentrated near the boundaries. There is some intracrystalline calcite present in which dolomite appears to be biting into calcite. There are some sulfides present and some remnant organic matter. Contains some intercrystalline quartz and some well rounded quartz and/or feldspar grains.

Interpretation:

The sulfides suggest the dolomite precipitated in a reducing environment. The subhedral texture suggests the dolomite precipitated from a dolomite supersaturated solution but, below critical supersaturation and below the critical roughening temperature which is approximately 50° C. The clear dolomite filling some molds suggests some primary dolomite precipitation occurred along with the replacement dolomitization. The intercrystalline quartz is authigenic, precipitating after dolomitization. The quartz\feldspar grains are detrital.

6 L

Classification:

Dunham - pelloidal biograinstone
Folk - pelloidal biosparite

Description:

Contains ooids, algae, echinoderms, brachiopods, foraminifera, compound grains, arthropods and pelloids set in a spar matrix. Most grains are highly micritized with some echinoderms also being partially silicified. The slide shows at least four sequences of graded bedding. Molds have been filled with spar and some micritized grains show spar rims. There is some organic matter and some well rounded quartz and/or feldspar grains present.

Interpretation:

The diverse fauna suggests deposition occurred in a normal marine environment. The cement rims on some grains and graded bedding suggests the grains were transported into the depositional area or autochthonous and churned up during the depositional event that produced the graded bedding. The quartz grains are detrital.

6 D

Classification:

Dunham - dolomitized biopackstone
Folk - dolomitized biomicrite
Sibley and Gregg - unimodal planar-s dolomite

Description:

Dolomite is unimodal and subhedral. There is non-mimic replacement of some grains and the grains are hard to identify. The dolomite appears dirty due to calcite inclusions. There is calcite present along dolomite crystal boundaries that contains a small amount of iron. Clearer, slightly coarser dolomite fills former grain molds. A minor amount of sulfides are present. Some intercrystalline quartz and some well rounded quartz and/or feldspar grains are present.

Interpretation:

The sulfides suggest deposition in a reducing environment. The subhedral texture suggests precipitation from a dolomite supersaturated solution, but below critical supersaturation and the critical roughening temperature of approximately 50° C. The clear, slightly coarser dolomite filling grain molds suggests precipitation of some primary dolomite. The intercrystalline quartz is authigenic, precipitating after some dolomitization. The quartz and/or feldspar grains are detrital.

7 L

Classification:

Dunham - partially dolomitized crinoid bearing mudstone
Folk - partially dolomitized crinoid bearing micrite

Description:

Sample is partially dolomitized and shows a good transition between limestone and dolomite. Sample contains echinoderms with minor amounts of brachiopods (?) and molluscs set in a mud matrix. There are some fractures present filled with coarse calcite and dolomite. In the transition from calcite to dolomite, dolomite is observed biting into the edges of some echinoderm grain edges and the finer micrite/spar. There are calcite inclusions present in the dolomite that decrease in abundance as one moves into the dolomitized zone. The dolomite contains some well developed sulfides.

Interpretation:

Depositional may have been normal marine as suggested by the fauna although it is hard to interpret from this slide. Dolomitization occurred in a reducing environment as indicated by the presence of sulfides.

7 D

Classification:

Dunham - dolomitized biopackstone
Folk - dolomitized biomicrite
Sibley and Gregg - nonplanar to planar-s dolomite

Description:

Dolomite is unimodal and mostly subhedral. Nonmimically replaced shell debris is observed which is hard to identify (echinoderms, brachiopods?). There are some dolomite-filled fractures present. The dolomite appears dirty due to the presence of calcite inclusions. The dolomite filling biomolds and fractures is clearer and slightly coarser than the replacement dolomite. There is some intercrystalline calcite present in the dolomite, where the dolomite appears to be biting into the calcite. Minor sulfides are present. There is some intercrystalline quartz, well rounded quartz and/or feldspar grains are present.

Interpretation:

Precipitation occurred in a reducing environment as indicated by the presence of sulfides. The subhedral texture suggests precipitation occurred from a dolomite supersaturated solution, but below critical supersaturation and the critical roughening temperature which is approximately 50° C. The clearer, slightly coarser dolomite that occurs in the biomolds and fractures suggests two dolomite precipitation events. The intercrystalline quartz is authigenic and precipitated after dolomitization. The intercrystalline quartz is authigenic, precipitating after dolomitization. The quartz/feldspar grains are detrital.

8 L portion

Classification:

Dunham - pelloidal biopackstone
Folk - pelloidal biomicrite

Description:

Highly micritized and contains echinoderms, arthropods (?), brachiopods (?), foraminifera (?), pellets and indistinguishable pelloidal material. Silicification has occurred along a fracture or stratigraphic plane. Some spar cement is observed filling pore space between micritized grains. In some places it appears micritized grains have "welded" together forming larger grains where former grain boundaries are indistinguishable. A few echinoderm, brachiopod and arthropod grains have not been micritized. There is some organic matter and well rounded quartz and/or feldspar grains present. The boundary between limestone and dolomite shows intense silicification that appears to follow depositional boundaries.

Interpretation:

The diverse fauna suggests deposition in a normal marine environment. The welded grains suggest compaction occurred before the pelloids were lithified. Silicification is a post depositional feature. The quartz and/or feldspar grains are detrital.

8 D portion

Classification:

Dunham - dolomitized biowackstone
Folk - dolomitized biomicrite
Sibley and Gregg - unimodal nonplanar dolomite

Description:

Dolomite is unimodal and mostly anhedral. There are some nonmimically replaced echinoderm and possibly brachiopod fragments. The dolomite appears dirty due to calcite inclusions. Dolomite that has nonmimically replaced the shell fragments is clearer. There are minor sulfides present. There is quartz present filling some intercrystalline pore space.

Interpretation:

The dolomite precipitated in a reducing environment as is suggested by the presence of minor sulfides. The anhedral texture of the dolomite suggests precipitation from a dolomite supersaturated solution, possibly above the critical supersaturation level or the critical roughening temperature which is approximately 50° C. The clear dolomite nonmimically replacing shell fragments is a primary precipitate. The quartz precipitated as an authigenic phase after dolomitization.

9 L

Classification:

Dunham - pelloidal biowackstone
Folk - pelloidal biomicrite

Description:

Contains micritized grains, foraminifera, mollusc, compound grains and other shell debris set in a micrite matrix. Some of the micritized grains have cement rims and some of the grains with cement rims also have micrite rims. There are fractures present, filled with coarse spar. Small quantities of organic matter also present. The micritized grains have irregular shapes. Some silicification of carbonate grains has occurred and some well rounded quartz and/or feldspar grains are present.

Interpretation:

The identifiable grains suggest deposition occurred in a normal marine environment. The irregular shape of the micritized grains suggests they are not fecal in origin, but skeletal. Silicification occurred after deposition. The quartz and/or feldspar grains are detrital.

9 D

Classification:

Dunham - dolomitized biowackstone
Folk - dolomitized biomicrite
Sibley and Gregg - unimodal planar-s dolomite

Description:

Dolomite is unimodal and subhedral. There are some molds and a few nonmimically replaced shell fragments present. The dolomite appears dirty due to calcite inclusions. The dolomite in the nonmimically replaced shell fragments is clearer. The dolomite appears to be biting into the intercrystalline calcite. There is some iron stains along dolomite crystal edges and minor sulfides and organic matter present. There is a minor amount of intercrystalline quartz and a few well rounded quartz and/or feldspar grains present.

Interpretation:

Dolomite precipitation occurred in a reducing environment, as suggested by the presence sulfides. The subhedral texture suggests precipitation occurred from a dolomite saturated solution but, below critical supersaturation and the critical roughening temperature of approximately 50° C. The clear dolomite nonmimically replacing the shell fragments is a primary precipitate. The intercrystalline quartz is authigenic, precipitating after dolomitization, while the quartz grains are detrital.

10 L

Classification:

Dunham - pelloidal biograinstone
Folk - pelloidal biospate

Description:

Contains micritized grains set in a spar matrix. Some grains are compound grains, intraclasts or echinoderm fragments while others may be brachiopods, foraminifera, ooids and pellets. There are some iron stains in the spar cement. Some grains have micritized rims. There are some square and rectangular molds present. Some silicification has occurred and some well rounded quartz and/or feldspar grains are present.

Interpretation:

The identifiable grains suggest deposition occurred in a normal marine setting. The silicification occurred after deposition. The quartz and/or feldspar grains are detrital.

10 D

Classification:

Dunham - dolomitized biopackstone
Folk - dolomitized biomicrite
Sibley and Gregg - unimodal planar-s dolomite

Description:

The dolomite is unimodal and subhedral. The dolomite appears dirty due to calcite inclusions. There are some molds and some nonmimically replaced shell fragments. The dolomite nonmimically replacing the shell fragments is slightly clearer. Dolomite appears to be biting into intercrystalline calcite. Quartz is present filling intercrystalline pore space.

Interpretation:

Dolomite did not precipitate in the sulfate reducing zone as indicated by the lack of sulfides or the thin section did not cut any sulfides. The subhedral texture suggests dolomite precipitated from a dolomite supersaturated solution, but below critical supersaturation and the critical roughening temperature of approximately 50° C. The clear dolomite of the nonmimically replaced shell fragments suggests it is a primary precipitate. The quartz precipitated as an authigenic phase after dolomitization.

12 L

Classification:

Dunham - pelloidal biograinstone
Folk - pelloidal biosparite

Description:

Contains highly micritized grains that include echinoderms, arthropods, brachiopods, intraclasts, compound grains, pellets and unidentifiable pelloids set in spar cement. Some grains have a spar rim, which is further rimmed by micrite. Some zones contain finer grains that are not continuous throughout the slide. Some micritized grains vary in size and shape. Partial silicification of some grains has occurred and some well rounded quartz and/or feldspar grains are present.

Interpretation:

The diverse fauna suggests deposition occurred in a normal marine environment. The varying size and shape of some micritized grains suggests they are not all of pelletal origin, but also skeletal. The silicification occurred after deposition and the quartz and/or feldspar grains are detrital.

12 D

Classification:

Dunham - dolomitized biopackstone
Folk - dolomitized biomicrite
Sibley and Gregg - unimodal planar-s dolomite

Description:

The dolomite is unimodal and subhedral. The dolomite appears dirty due to the presence of calcite inclusions. Nonmimically replaced shell fragments are present. Some are molds that are only partially filled with with a clearer dolomite. Identification of the organisms that produced the molds is difficult. There are minor sulfides and organic matter present. Quartz is present filling intercrystalline pore space.

Interpretation:

The dolomite precipitated in a reducing environment as is indicated by the presence of minor sulfides. The subhedral texture suggests the dolomite precipitated from a dolomite supersaturated solution, but below critical supersaturation and the critical roughening temperature of approximately 50° C. The clearer dolomite observed filling molds suggests it precipitated from solution. The quartz is authigenic, precipitating after dolomitization.

13 L

Classification:

Dunham - pelloidal biograinstone
Folk - pelloidal biosparite

Description:

Sample contains micritized and partially micritized grains that include echinoderms, brachiopods, arthropods, intraclasts and corals set in a spar matrix. The totally micritized grains vary in size and shape although some appear pelletal. The grains are tightly packed in some places resulting in an almost totally micritic appearance. There is some organic matter and well rounded, quartz and/or feldspar grains are present. Some silicification of carbonate grains has occurred. An identifiable feldspar grain is present.

Interpretation:

The diverse fauna suggests a normal marine depositional environment. The varying size and shape of the pelloids suggests a skeletal origin for most, although some may be pellets. Silicification occurred after deposition. The quartz and/or feldspar grains are detrital.

13 D

Classification:

Dunham - Dolomitized biopackstone
Folk - Dolomitized biosparite
Sibley and Gregg - unimodal planar-s dolomite

Description:

The dolomite is unimodal and subhedral and appears dirty due calcite inclusions. Dolomite is observed biting into calcite and "floating" in calcite. There are minor sulfides present and some organic matter. Some nonmimically replaced skeletal fragments may be present. Quartz is present filling intercrystalline pores.

Interpretation:

The dolomite precipitated in a reducing environment as suggested from the presence of minor sulfides. The subhedral texture suggests dolomite precipitated from a dolomite supersaturated solution, but below critical supersaturation and the critical roughening temperature of approximately 50° C. The quartz is authigenic, precipitating after dolomitization.

APPENDIX B QMAS Theory

The following summary of the theory of the QMAS system and the analytical methods used to obtain data for the QMAS system is condensed from Slaughter (1985). The QMAS System is a computer program developed at Crystal Research Laboratories in Lander, Wyoming which integrates bulk chemical analysis, CO₂/H₂O analysis and x-ray diffraction data through linear programming to determine the mineralogy quantitatively and chemical composition of each mineral of a sample. To obtain quantitative mineralogy and compositions, two linear programming problems must be solved.

Linear programming problems are based on optimization of an objective function subject to constraints. An example is as follows:

Optimize the objective function

$$f_1 = c_1x_1 + c_2x_2 + \dots + c_nx_n, \quad (1)$$

subject to the constraints

$$\begin{array}{l} a_{11}x_1 + a_{12}x_2 + \dots + a_{1n}x_n \leq b_1 \\ a_{21}x_1 + a_{22}x_2 + \dots + a_{2n}x_n \leq b_2 \\ \vdots \\ a_{m1}x_1 + a_{m2}x_2 + \dots + a_{mn}x_n \leq b_m \end{array} \quad (2a)$$

$$x_i \geq 0 \quad (i=1, \dots, n), \quad (2b)$$

where the values a, b, and c are known constants. The inequality expressions are constraints (2a) shown as "less-than-or-equal-to" (LTE) expressions here, although "greater-than-or-equal-to" (GTE) expressions may be used by multiplying both sides of the inequality (2a) by -1. The inequalities (2) describe a closed set of solutions which, if the

set is also bounded, will have at least one maximum and one minimum and, therefore, optimal feasible solutions over the solution set.

Linear programming usually uses constraints in the form of linear equalities. "Slack" variables are introduced into each LTE to convert it to a linear equality. The slack variable represents the value which, when added to the left side of each constraint, would transform the inequality to a linear equality. Thus, a slack variable is added to each constraint to represent the sum needed to become a linear equality. The slack variables are also included in the objective function because the objective function must evaluate all variables.

After conversion of the constraints to linear equalities through the addition of slack variables, the general problem appears as follows:

optimize

$$f_I = c_1x_1 + c_2x_2 + \dots + c_nx_n + 0_{x_{n+1}} + \dots + 0_{x_{n+m}} \quad (3)$$

subject to

$$\begin{aligned} a_{11}x_1 + a_{12}x_2 + a_{13}x_3 + \dots + a_{1n+m}x_{n+m} &= b_1 \\ a_{12}x_1 + a_{22}x_2 + a_{23}x_3 + \dots + a_{2n+m}x_{n+m} &= b_2 \\ &\vdots \\ &\vdots \\ a_{m1}x_1 + a_{m2}x_2 + a_{m3}x_3 + \dots + a_{mn+m}x_{n+m} &= b_m \end{aligned} \quad (4a)$$

$$x_i \geq 0, (i=1, \dots, n+m) \quad (4b)$$

To eliminate the effect of the slack variables on the optimization function, they are multiplied by zero.

Constraints of the GTE form would be transformed into linear equalities by the addition of "surplus" variables. Surplus variables represent the sums which, when added to the left side of the inequality constraint, causes both sides of the constraints to be equal. Surplus variables are always negative because GTE constraints require a reduction in value of the

left side to produce a linear equality. The Simplex Method of solution for the general linear programming problem can be used if the general linear programming problem is written as described in any linear programming text.

The first linear programming problem (Problem I) determines the amounts of minerals of known composition. The second problem (Problem II) determines the mineral amounts and compositions of minerals of variable compositions. To determine the amounts of minerals of known composition, an objective function and constraints describing the problem must be established. The weight fraction of an element in a rock attributed to a specific mineral is equal to the product of the weight fraction of the mineral in the rock times the weight fraction of an element or oxide in the mineral. The weight fraction of that specific element in the whole sample will be less than or equal to the sum of similar products for all minerals in the sample. The weight fraction of the element in the total sample is less than or equal to the total, because it is likely that other minerals present in minor amounts and amorphous phases are contributing to the chemical composition. Thus, the expression for the weight fraction of a specific element in the total sample is

$$\sum_{j=1}^n a_{ij}x_j \leq B_i \quad (5)$$

where a_{ij} is the weight fraction of mineral j , x_j is the weight fraction of mineral j in the samples, and B_i is the weight fraction of element i in the sample. The sum of the weight fractions of all the minerals in the sample will be equal to (or less than) one and expressed as

$$\sum_{j=1}^n x_j \leq 1 \quad (6)$$

The objective function of this model is

$$\sum_{j=1}^n -1(x_j) = f_I \quad (7)$$

If the chemical analysis is accurate and the chemical compositions of all the minerals are known, maximization of the objective function gives the amounts of each mineral in the rock.

Linear programming Problem I cannot give mineral amounts accurately for minerals of variable compositions. By altering the objective function and constraints from Problem I by deleting the column vectors of the k th mineral and inserting new ones gives Problem II with the following new objective function and constraints:

optimize

$$f_{II} = c_1x_1 + c_2x_2 + \dots + c_{k-1}x_{k-1} + A_{1k}X_k + A_{2k}X_k + \dots + A_{mk}X_k + c_{k+1}x_{k+1} + \dots + c_nx_n \quad (8)$$

subject to

$$\begin{aligned} a_{11}x_1 + a_{12}x_2 + \dots + a_{1k-1}x_{k-1} + A_{1k}X_k + a_{1k+1}x_{k+1} + \dots + a_{1n}x_n &\leq b_1 \\ a_{21}x_1 + a_{22}x_2 + \dots + a_{2k-1}x_{k-1} + A_{2k}X_k + a_{2k+1}x_{k+1} + \dots + a_{2n}x_n &\leq b_2 \\ \vdots &\vdots \\ a_{m1}x_1 + a_{m2}x_2 + \dots + a_{mk-1}x_{k-1} + A_{mk}X_k + a_{mk+1}x_{k+1} + \dots + a_{mn}x_n &\leq b_m \end{aligned} \quad (9a)$$

$$x_i, X_k, A_{ik} \geq 0 \quad (9b)$$

where A_{ik} is the atomic fraction of element i in the k th mineral. The maximum possible atomic fraction of the k th mineral in the sample is X_k defined by

$$x_k + (100-f_l)$$

from the solution of Problem I. The Simplex Method for solving determines the optimum values of A_{ik} and thus, an optimum composition for the k th mineral.

Convergence of alternate iterations of linear programming problems I and II produces an optimal set of mineral amounts and compositions for all minerals whose compositions are determined. Combining Problems I and II works well except for degeneracy when two or more minerals of the same composition or element type are present (i.e. some compositions of microcline, orthoclase and sanidine). X-Ray analysis, another method of yielding, constraints is necessary in such situations.

DEFINITION OF CONSTRAINTS FOR PROBLEM I AND II

Constraints for Problem I - X-Ray Diffraction Intensity

For Problem I, constraints are quantitative mineral estimates by x-ray diffraction or other methods. X-Ray diffraction intensity constraints can be used to specify amounts of minerals in a rock and to constrain the compositional range of a mineral.

Quantitative amounts of some minerals in a bulk sample can be determined by x-ray diffraction from standard curves by ratioing diffraction intensities to internal standard intensities. Constraints of the LTE and GTE type result:

$$\begin{aligned}x_j &\leq d_1; \\x_j &\geq d_2,\end{aligned}\tag{10}$$

where d_1 and d_2 are the determined amounts of the minerals plus and minus the expected analytical error. Expression (10) adds important constraints and aids in determination of amorphous phases of known composition by reducing the number of unknowns to be determined by chemistry.

Although the amount constraints may have large ranges between GTE and LTE constraints, they are useful in preventing false solutions. Chemical analysis provides more rigorous constraints and when coupled with estimated mineral amounts from x-ray diffraction, allows for specification of amorphous phases. This is especially effective for silica (opal) and allophane specification and even permits determining the composition of these phases.

Constraints for Problem II from Compositional, Structural and Charge Balance Considerations

Ranges of elemental compositions are available for minerals based on published chemical analyses. For example, montmorillonite can have between zero and 0.7 Mg atoms substituting for Al in the octahedral layer per ten oxygen formula. The constraints are

$$N_{\text{Mg}} \leq .7,$$

$$N_{\text{Mg}} \geq 0.0.$$

Compositional constraints may contain more than one element and may apply to a family of minerals. For example, using trend analysis on the smectite group,

$$\text{Al}_2\text{O}_3 \leq 33.50 - .6551 (\text{Fe}_2\text{O}_3 + \text{FeO} + \text{MgO}),$$

$$\text{Al}_2\text{O}_3 \geq 19.65 - .6551 (\text{Fe}_2\text{O}_3 + \text{FeO} + \text{MgO}),$$

where oxides are in weight percentage.

Elemental site occupancy in a mineral structure is limited by structural and charge balance constraints. In montmorillonite, there are two octahedral sites per ten oxygen formula which are occupied dominantly Al, Fe⁺³ and Mg with traces of other elements. Al and possibly small amounts of Fe⁺³ substitute for Si in the tetrahedral layer. Ca and Na primarily compensate for the charge imbalance caused by Mg substituting for Al in the octahedral layer and Al substituting for Si in the tetrahedral layer. For a ten oxygen formula, the following formulas constrain the composition and charge balance:

$$N_{\text{Al}} = (4 - N_{\text{Si}}) + 2 - N_{\text{Mg}} - N_{\text{Fe}} \text{ and}$$

$$N_{\text{Ca}/2} + N_{\text{Na}} = (4 - N_{\text{Si}}) + N_{\text{Mg}} + N_{\text{Fe}+2},$$

where N is the number of moles of atoms of the subscript element. The above equalities become LTE and GTE inequalities with small allowable ranges. This allows small amounts of K, Mg and Sr to substitute for Ca and Na and/or a few vacancies or excess atoms in the octahedral layer.

In problem II d-spacing constraints can further constrain composition, because substitutions in clays and other minerals can be related to observed x-ray diffraction d-

spacings. Microcline, for example, never has the ideal KAlSi_3O_8 . Up to 1/3 of K can be substituted for by Na, which changes microclines main diffractions because of the smaller Na ion substituting in the structure. The d-spacing establishes a restricted range of substitution that can be expressed as an experimental constraint. Diffraction overlaps sometimes do not allow d-spacing constraints to be used. Calcite to Mg-calcite, dolomite to ferroan dolomite to ankerite, siderite to Mg-siderite, chlorite, nontronite, opal-c (cristobalite) and opal-t (tridymite) are a few clay and associated minerals and mineral groups allowing d-spacing constraints. D-Spacing constraints are simple, as in the example of (0k0) spacings for chlorite which determines limits on Fe^{+2} content in the octahedral layer. The chlorite (060) reflection ranges from 1.53 Å to 1.55 Å. Using the relation of Radslovich (1962):

$$N_{\text{Fe}^{+2}} = 200.00 * d(060) - 307.66 \pm .95.$$

The $\pm .95$ defines the LTE and GTE constraints. D-Spacing constraints are formulated in the calculation so that only the d-spacing must be specified, but they are mineral specific. D-Spacing constraints can be included explicitly in the linear programming matrix or tableau, or they can be used to modify the elemental range constraints for specific elements, which reduces the size of the tableau. D-Spacing constraints must appear in the tableau if they are a function of more than one element.

APPENDIX C

Mass Balance Calculations of Carbon Isotope Values in Organogenic Dolomites

Calculations of $\delta^{13}\text{C}$ values for dolomites in Tables 10 and 11 were based on 1m^3 of sediment with porosity ranging from 30% to 70% and initial organic content of 3%, 5%, 8%, 10%, 12%, 15%, 20% and 25%. The carbon content of organic matter in sediments for the calculations was estimated from analysis of Huc, et al., (1978) on organic matter in the Black Sea to be 56%. Rashid (1985) estimated that 30% to 40% of the organic matter initially deposited in sediments is destroyed by bacterial sulfate reduction. The calculations were done assuming 40% of the carbon initially present in the sediments was bacterially oxidized to CO_2 . The moles of CO_3^{-2} produced from bacterial sulfate reduction and the moles of CO_3^{-2} available from the precursor limestone of various porosity in 1m^3 of sediment were then used to calculate the mole percent CO_3^{-2} contributed to the dolomite forming by replacement of the original limestone. The density used for calcite to determine the number of moles of CO_3^{-2} available from the limestone was 2.71 g/cm^3 . Similar calculations were done to determine the number of moles of CO_3^{-2} available for dolomitization after 50% and 25% of the CO_3^{-2} produced by bacterial sulfate reduction was reduced to methane by bacterial CO_2 reduction. The moles of CO_3^{-2} in the pore waters in equilibrium with the limestone is negligible and not included in the calculations. The $\delta^{13}\text{C}$ values for CO_2 used for the calculations are -20‰ (Presley and Kaplan, 1968) from sulfate reduction and $+15\text{‰}$ and -7‰ , respectively, for CO_2 left after CO_2 reduction (Nissenbaum, et al., 1972).

Sample calculations are summarized below.

Moles of carbonate from precursor limestone:

1 m^3 sediment x 70% porosity = $.70\text{ m}^3$ of pore space or $.30\text{ m}^3$ of sediment

$.30 \times 10^6\text{ cm}^3$ sediment x 2.71 g/cm^3 = 8.13×10^5 g of limestone

8.13×10^6 g of limestone / 100 g/mole = 8.12×10^3 moles limestone = 8.12×10^3 moles CO_3^{-2}

Moles of carbonate from organic matter during sulfate reduction:

$.03 \times 10^6\text{ cm}^3$ organic matter (3%) x 1 g/cm^3 = 30,000 g organic matter (OM)

30,000 g OM x .56 g carbon/g OM = 16,800 g carbon

16,800 g carbon x .40 g carbon consumed in sulfate reduction/g carbon = 6720 g carbon
consumed during sulfate reduction

6720 g carbon / 12.0 g/mole = 560 moles CO_3^{-2} produced during sulfate reduction

Moles of carbonate from pore waters in equilibrium with limestone (calcite):

At equilibrium, $\text{CaCO}_3 = \text{Ca}^{+2} + \text{CO}_3^{-2}$ $k_{\text{eq}} = 10^{-6.23} = (\text{Ca}^{+2})(\text{CO}_3^{-2})$

This implies $(\text{CO}_3^{-2}) = 7.67 \times 10^{-4}$ moles/liter x .67 liters gives 5.14×10^{-4} moles of carbonate from pore waters before sulfate reduction which is negligible in these calculations.

Thus, for limestone with 70% initial porosity, 8.12×10^3 moles of carbonate are available from limestone (93.5% of total moles of carbonate) for dolomitization and 560 moles of carbonate from organic matter (6.5% of total moles of carbonate) are available for dolomitization. This is 8680 total moles of carbonate. Assuming an initial $\delta^{13}\text{C}$ for the limestone of 1‰ and for the CO_3^{-2} from sulfate reduction of -20‰ of 3% OM, the $\delta^{13}\text{C}$ of the dolomite formed by replacement would be -0.36‰. The final calculation is

$\delta^{13}\text{C} = (.065 \times -20\text{‰}) + (.935 \times 1\text{‰}) = -0.36\text{‰}$ for the dolomite.

Similar calculations were done for different initial rock $\delta^{13}\text{C}$ values, organic contents and sediment porosities during sulfate reduction and methanogenesis.

Table 10: Calculated carbon isotope values in carbonate rocks for various amounts of organic matter and carbonate rock porosity for rock $\delta^{13}C = 1\text{‰}$

Rock Moles CO_2 (10^3)	Sulfate Reduction Mole % CO_2 (20‰)	$\delta^{13}C$	50% CO_2 Reduction Mole % CO_2 (19‰)	$\delta^{13}C$	50% CO_2 Reduction Mole % CO_2 (7‰)	$\delta^{13}C$
8.12x10 ³ 30% rock	3.3 (3)	0.32	1.7	1.24	2.5	0.80
	5.3 (5)	-0.11	2.7	1.38	4.0	0.68
	8.2 (8)	-0.72	4.3	1.60	6.3	0.50
	10.1 (10)	-1.12	5.3	1.74	7.7	0.40
	11.8 (12)	-1.48	6.3	1.88	9.1	0.27
	14.4 (15)	-2.02	7.7	2.08	11.2	0.10
	18.3 (20)	-2.84	10.1	2.41	14.4	-0.15
	21.9 (25)	-3.60	12.3	2.72	17.3	-0.38
	2.5	0.48	1.3	1.18	1.9	0.85
	4.0	0.16	2.1	1.29	3.1	0.75
1.08x10 ⁴ 40% rock	6.3	-0.32	3.3	1.46	4.8	0.62
	7.8	-0.64	4.0	1.56	5.9	0.53
	9.2	-0.93	4.8	1.67	7.0	0.44
	11.2	-1.35	5.9	1.83	8.6	0.31
	14.4	-2.02	7.8	2.09	11.2	0.10
	17.3	-2.63	9.5	2.33	13.6	-0.09
	2.0	0.58	1.0	1.14	1.5	0.88
	3.3	0.31	1.7	1.24	2.5	0.80
	5.1	-0.07	2.6	1.36	3.9	0.69
	6.3	-0.32	3.3	1.46	4.8	0.62
1.35x10 ⁴ 50% rock	7.5	-0.57	3.9	1.55	5.7	0.54
	9.2	-0.93	4.8	1.67	5.7	0.44
	11.9	-1.50	6.3	1.88	7.0	0.26
	14.4	-2.02	7.8	2.09	11.2	0.10
	1.7	0.64	0.8	1.11	1.2	0.90
	2.7	0.43	1.4	1.20	2.1	0.83
	4.3	0.10	2.2	1.31	3.2	0.74
	5.3	-0.11	2.7	1.38	4.0	0.68
	6.3	-0.32	3.3	1.46	4.8	0.62
	7.7	-0.62	4.0	1.56	5.9	0.53
1.625x10 ⁴ 60% rock	10.1	-1.12	5.3	1.74	7.7	0.38
	12.3	-1.58	6.5	1.91	9.5	0.24
	1.9	0.70	0.7	1.10	1.1	0.91
	2.3	0.52	1.2	1.17	1.8	0.86
	3.7	0.22	1.9	1.27	2.8	0.78
	4.6	0.03	2.4	1.34	3.5	0.72
	5.6	-0.18	2.8	1.39	4.1	0.67
	6.7	-0.41	3.5	1.49	5.1	0.59
	8.8	-0.85	4.6	1.64	6.7	0.46
	10.7	-1.25	5.7	1.80	8.3	0.34
1.89x10 ⁴ 70% rock						

Table 11: Calculated carbon isotope values in carbonate rocks for various amounts of organic matter and carbonate rock porosity and $\delta^{13}C = 3\text{‰}$.

Rock Moles CO_3^{2-} (3‰)	Initial Volume Percent OM	Sulfate Reduction		50% CO_2 Reduction		25% CO_2 Reduction	
		Mole % CO_3^{2-} (-20‰)	$\delta^{13}C$	Mole % CO_3^{2-} (15‰)	$\delta^{13}C$	Mole % CO_3^{2-} (-7‰)	$\delta^{13}C$
8.12x10 ³ 30% rock	3	6.5	1.50	2.2	3.26	4.9	2.51
	5	10.3	0.90	5.2	3.62	7.7	2.23
	8	15.5	-0.56	7.7	3.92	11.6	1.84
	10	18.7	-1.30	9.3	4.12	14.0	1.60
	12	21.6	-1.97	10.8	4.30	16.2	1.38
1.08x10 ⁴ 40% rock	15	25.0	-2.89	12.8	4.54	18.7	1.13
	20	31.5	-4.24	15.7	4.88	23.6	0.64
	25	36.5	-5.39	18.2	5.19	27.4	0.26
	3	4.9	1.87	2.4	3.29	3.7	2.63
	5	7.9	1.18	3.9	3.47	5.9	2.41
1.35x10 ⁴ 50% rock	8	12.1	0.22	6.0	3.72	9.1	2.09
	10	14.7	-0.38	7.3	3.88	11.0	1.90
	12	17.2	-0.96	8.6	4.03	12.9	1.71
	15	20.6	-1.74	10.3	4.24	15.4	1.46
	20	25.7	-2.91	12.8	4.54	19.3	1.07
1.63x10 ⁴ 60% rock	25	30.1	-3.93	15.0	4.80	22.6	0.74
	3	4.0	2.08	2.0	3.24	3.0	2.70
	5	6.5	1.50	3.2	3.38	4.9	2.51
	8	10.0	0.70	5.0	3.60	7.5	2.25
	10	12.1	0.22	6.0	3.72	9.1	2.09
1.89x10 ⁴ 70% rock	12	14.2	-0.27	7.1	3.85	10.6	1.94
	15	17.2	-0.96	8.6	4.03	12.9	1.71
	20	21.6	-1.97	10.8	4.30	16.2	1.38
	25	25.7	-2.91	12.8	4.54	19.3	1.07
	3	3.3	2.24	1.6	4.92	2.5	2.75
1.89x10 ⁴ 70% rock	5	5.4	1.76	2.7	3.32	4.0	2.60
	8	8.4	1.07	4.2	3.50	6.3	2.37
	10	10.3	0.63	5.1	3.61	7.7	2.23
	12	12.1	0.22	6.0	3.72	9.1	2.09
	15	14.6	-0.36	7.3	3.88	10.9	1.91
1.89x10 ⁴ 70% rock	20	18.6	-1.28	9.3	4.12	13.9	1.61
	25	22.2	-2.11	11.1	4.33	16.6	1.34
	3	2.9	2.33	1.4	3.17	2.2	2.78
	5	4.7	1.92	2.3	3.28	3.5	2.65
	8	7.3	1.32	3.6	3.43	5.5	2.45
1.89x10 ⁴ 70% rock	10	9.0	0.93	4.5	3.54	6.7	2.33
	12	11.6	0.56	5.3	3.64	7.9	2.21
	15	12.9	0.03	6.4	3.77	9.7	2.03
	20	16.5	-0.79	8.2	3.98	12.4	1.76
	25	19.8	-1.55	9.9	4.19	14.8	1.52